ORGANOMETALLICS

Article

Cite This: *Organometallics* XXXX, XXX, XXX−XXX

Cobalt POCOP Pincer Complexes via Ligand C−H Bond Activation with $Co_2(CO)_8$: Catalytic Activity for Hydrosilylation of Aldehydes in an Open vs a Closed System

Yingze Li, Jeanette A. Krause, and Hairong Guan*

Department of Chemistry, University of Cincinnati, P.O. Box 210172, Cincinnati, Ohio 45221-0172, United States

Supporting Information

ABSTRACT: A series of cobalt POCOP pincer complexes with the formulas {2,6-(^{i}Pr$_2$PO)$_2$-4-R′-C$_6$H$_2$}Co(CO)$_2$ (R′ = H (**1a**), NMe$_2$ (**1b**), OMe (**1c**), CO$_2$Me (**1d**)), {2,6-(Ph$_2$PO)$_2$C$_6$H$_3$}Co(CO)$_2$ (**1e**), and {2,6-(^{t}Bu$_2$PO)$_2$C$_6$H$_3$}Co(CO) (**2f**) have been synthesized through C−H bond activation of the corresponding pincer ligands with $Co_2(CO)_8$. These complexes have been demonstrated to catalyze the hydrosilylation of PhCHO with (EtO)$_3$SiH, which exhibits an induction period and the decreasing reactivity order **1b** > **1c** > **1a** > **1d** > **1e**. The catalytic protocol can be applied to various aldehydes with turnover numbers of up to 300. The CO ligands in the dicarbonyl complexes have been shown to exchange with ^{13}CO at room temperature and partially dissociate from cobalt at high temperatures. Substitution of CO by *tert*-butyl isocyanide has been accomplished with **1a** at 50−80 °C, resulting in the formation of {2,6-(^{i}Pr$_2$PO)$_2$C$_6$H$_3$}Co(^{t}BuNC)(CO) (**3a**) and {2,6-(^{i}Pr$_2$PO)$_2$C$_6$H$_3$}Co(^{t}BuNC)$_2$ (**4a**). The catalytic reactions are more efficient when they are carried out in an open system or if the catalysts are preactivated by the aldehydes. The structures of **1a−e**, **3a**, and **4a** have been studied by X-ray crystallography.

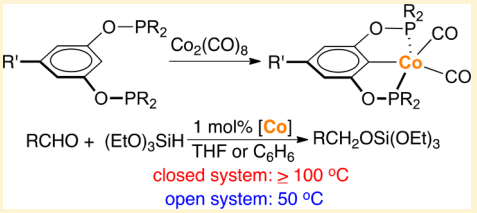

INTRODUCTION

Bis(phosphinite)-based pincer complexes, which are also known as POCOP pincer complexes, have been explored extensively as catalysts for a broad range of applications.[1] Some of the prominent examples are iridium-catalyzed dehydrogenation processes,[2] palladium-catalyzed C−C bond forming reactions,[3] and rhodium-catalyzed C−S coupling of aryl halides with thiols.[4] In our research group, we have focused on using inexpensive, earth-abundant metals to build pincer complexes for various catalytic transformations, especially for the reduction of carbonyl compounds.[5] Considering that employing expensive ligands would defeat the purpose of utilizing inexpensive metals, we are particularly interested in the POCOP pincer systems because the ligands can be readily synthesized at a relatively low cost. Our previous work in this research area has led to the discovery of nickel-catalyzed reduction of CO_2 with boranes,[6] nickel-catalyzed cyanomethylation of aldehydes,[7] and iron-catalyzed dehydrogenation of ammonia−borane.[8] Mechanistic investigations have suggested that both nickel and iron maintain the +2 oxidation state during the catalytic cycles. Given that many catalytic reactions do require a change in metal oxidation state, we sought to study the potential use of cobalt POCOP pincer complexes as homogeneous catalysts because of the possible involvement of Co(I)/Co(III) cycles.

Cobalt complexes supported by a POCOP pincer ligand are rare in the literature and, to the best of our knowledge, have not been reported for any catalytic applications. Related pincer complexes of Ir,[9] Rh,[10] Pt,[11] Pd,[11b−g,12] and Ni[11d−g,12f,13] have been routinely synthesized via cyclometalation of the POCOP pincer ligands with the corresponding metal halide salts, including those bearing labile ligands such as MeCN, R$_2$S, and 1,5-cyclooctadiene. However, applying such a strategy to cobalt led to unsatisfactory yields, as described by Heinekey et al.[14,15] and confirmed in our laboratory. Therefore, lithiation of an iodo-substituted POCOP pincer ligand followed by the addition of CoI_2·THF has been developed as an alternative route to {2,6-(^{t}Bu$_2$PO)$_2$C$_6$H$_3$}CoI (eq 1),[14] from which many

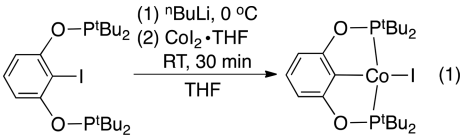

{2,6-(^{t}Bu$_2$PO)$_2$C$_6$H$_3$}Co derivatives can be made.[16] This lithiation method is also applicable to the synthesis of cobalt complexes supported by other pincer ligands, including [2,6-(Me$_2$NCH$_2$)$_2$C$_6$H$_3$]$^-$,[17] [2,6-(Ph$_2$PCH$_2$)$_2$C$_6$H$_3$]$^-$,[18] and [2,6-(^{i}Pr$_2$PNMe)$_2$C$_6$H$_3$]$^-$.[19]

In our experience with POCOP pincer complexes, the P−O bonds are vulnerable to attack by nucleophiles or bases, especially when the phosphorus substituents are smaller than *tert*-butyl groups (e.g., isopropyl and cyclopentyl groups).[6c,20] Thus, we were more intrigued by the method developed by Li and co-workers, who successfully activated the pincer central C−H bonds with MeCo(PMe$_3$)$_4$ (eqs 2 and 3)[21,22] or

Received: April 28, 2018

DOI: 10.1021/acs.organomet.8b00273
Organometallics XXXX, XXX, XXX−XXX

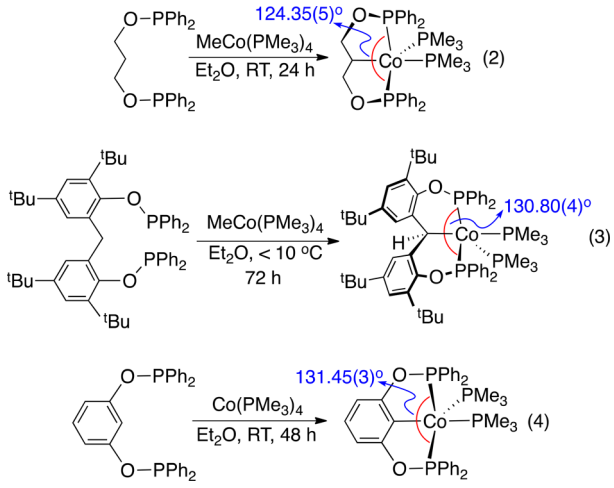

$Co(PMe_3)_4$ (eq 4).[23] The above procedures prompted us to examine if the C−H bond activation protocol could be broadly applied to other POCOP pincer systems. Our attempts to synthesize $\{2,6\text{-}(^iPr_2PO)_2C_6H_3\}Co(PMe_3)_2$ under similar conditions were, however, unsuccessful. A close inspection of the structures for the complexes shown in eqs 2−4 suggests that the steric pressure exerted by the PMe_3 ligands forces the POCOP pincer core to distort from planarity and the P−Co−P angle to contract from its "natural bite angle". For comparison, the average P−M−P angle of POCOP pincer complexes is 160.6°[24] and the P−Co−P angles of closely related cobalt pincer complexes fall within the range of 152.3−167.0°.[14−16,19] On the basis of this analysis, we suspected that the rigidity of the $[2,6\text{-}(^iPr_2PO)_2C_6H_3]^-$ pincer backbone and the steric crowding (increased from phenyl to isopropyl) would make the C−H bond activation less favorable.

In searching for more effective strategies to gain access to the $\{2,6\text{-}(^iPr_2PO)_2C_6H_3\}Co$ pincer platform, we have identified the commercially available $Co_2(CO)_8$ as another source of low-valent cobalt to activate the central C−H bonds of POCOP pincer ligands. We have also demonstrated that the resulting cobalt dicarbonyl complexes, when appropriately activated, are capable of catalyzing the hydrosilylation of aldehydes. The synthesis, structural characterization, and catalytic studies of these new cobalt POCOP pincer complexes, including some preliminary mechanistic data, are reported in this paper.

RESULTS AND DISCUSSION

Synthesis and Structures of Cobalt POCOP Pincer Complexes. Cobalt-promoted C−H bond activation dates back to the 1950s, when Murahashi reported $Co_2(CO)_8$-catalyzed cyclocarbonylation of *N*-benzylideneaniline (eq 5)[25]

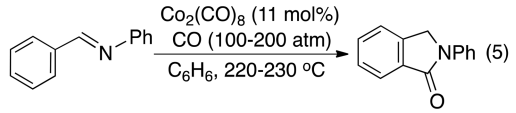

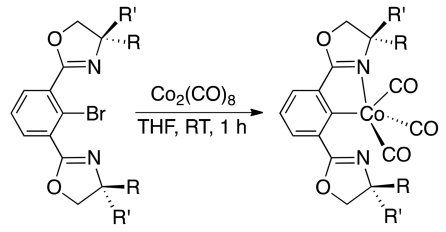

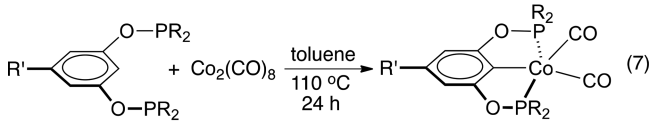

1a: R = ^{i}Pr, R' = H
1b: R = ^{i}Pr, R' = NMe_2
1c: R = ^{i}Pr, R' = OMe
1d: R = ^{i}Pr, R' = CO_2Me
1e: R = Ph, R' = H

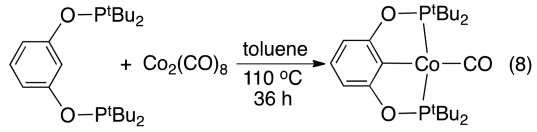

2f

and azobenzene.[26] In terms of stoichiometric reactions, $Co_2(CO)_8$ has been shown to react with a brominated bis(oxazolinyl)phenyl ligand to form a cobaltacycle (eq 6),[27] presumably through a dinuclear oxidative addition process. Inspired by these studies, we decided to test the feasibility of using $Co_2(CO)_8$ to activate POCOP pincer C−H bonds. After extensive optimization, it was found that refluxing $Co_2(CO)_8$ with 2.5 equiv of $1,3\text{-}(^iPr_2PO)_2C_6H_4$ for 24 h afforded $\{2,6\text{-}(^iPr_2PO)_2C_6H_3\}Co(CO)_2$ (**1a**), which was isolated as a bright yellow solid in 76% yield (eq 7).[28] Following the same procedures, the analogous cobalt POCOP pincer complexes bearing a para substituent (NMe_2, OMe, or CO_2Me) or Ph_2P donors (instead of $^iPr_2P$ donors) were also successfully obtained in good yields (71−95%). Interestingly, replacing the isopropyl with *tert*-butyl groups as the phosphorus substituents led to further CO expulsion (eq 8); the isolated pincer complex **2f** was identified as the previously known $\{2,6\text{-}(^tBu_2PO)_2C_6H_3\}Co(CO)$.[16] Loss of CO from the dicarbonyl species $\{2,6\text{-}(^tBu_2PO)_2C_6H_3\}Co(CO)_2$ (**1f**) was reported to occur at 70 °C.[16]

The mechanistic details for the reactions in eqs 7 and 8 are unclear to us. We propose that dinuclear oxidative addition of

Table 1. Selected Spectroscopic Data for the Cobalt Dicarbonyl Complexes

complex	R′	R	δ_{CO}[a]	δ_{ipsoC}[a]	δ_{metaC}[a]	δ_{paraC}[a]	ν_{CO} (cm^{-1})[e]
1b	NMe_2	^{i}Pr	205.95 (m)	121.94 (m)[d]	90.77 (t)	150.88 (s)	1965, 1906
1c	OMe	^{i}Pr	205.57 (t)	126.64 (t)	91.63 (t)	159.41 (s)	1965, 1908
1a	H	^{i}Pr	205.40 (m)[b]	138.13 (t)	104.09 (t)	124.74 (s)	1966, 1912
1d	CO_2Me	^{i}Pr	204.63 (t)	149.57 (t)	104.89 (t)	127.08 (s)	1975, 1919
1e	H	Ph	203.40 (m)[c]	137.52 (t)	105.93 (t)	126.15 (s)	2001, 1936

[a]In CD_2Cl_2. Abbreviations: m = multiplet; t = triplet; s = singlet. [b]In C_6D_6, δ_{CO} 205.71 (t, J_{P-C} = 15.4 Hz). [c]In C_6D_6, δ_{CO} 203.65 (t, J_{P-C} = 10.1 Hz). [d]In C_6D_6, δ_{ipsoC} 121.99 (t, J_{P-C} = 22.2 Hz). [e]For solid samples.

DOI: 10.1021/acs.organomet.8b00273
Organometallics XXXX, XXX, XXX−XXX

the POCOP pincer ligands at cobalt (with concomitant dissociation of CO) forms the desired pincer complexes and $HCo(CO)_4$. The latter complex is known to decompose into H_2 and $Co_2(CO)_8$,[29] which in this case allows a full utilization of the available cobalt. Consistent with this mechanistic proposal, H_2 was detected (by ^1H NMR spectroscopy) from the reaction of 1,3-$(^iPr_2PO)_2C_6H_4$ with $Co_2(CO)_8$ carried out at 110 °C in C_6D_6.

Complexes **1a−e** were characterized by NMR, IR, and elemental analysis. Key spectroscopic data are summarized in Table 1. For the isopropyl derivatives (**1a−d**), each shows only one set of $CH(CH_3)_2$ and $CH(CH_3)_2$ resonances, suggesting that in solution these molecules have C_{2v} symmetry. In CD_2Cl_2, the CO resonance appears as a triplet for **1c** (J_{P-C} = 13.1 Hz) and **1d** (J_{P-C} = 14.1 Hz) but a poorly resolved multiplet for **1a,b,e**, likely caused by the quadrupolar ^{59}Co nucleus. The resolution is improved for **1a,e** when C_6D_6 is used as the NMR solvent, resulting in triplets at 205.71 ppm (J_{P-C} = 15.4 Hz) and 203.65 ppm (t, J_{P-C} = 10.1 Hz), respectively. However, the CO resonance for **1b** remains an unresolved multiplet. The *ipso* carbon was not located for the previously reported *tert*-butyl analogue **1f** as well as the monocarbonyl complex **2f**.[16] In contrast, it was observed as a triplet for both the isopropyl (**1a−d**) and phenyl (**1e**) derivatives with a phosphorus−carbon coupling constant of 21.2−24.4 Hz.

The electronic effect of the para substituent on the chemical shifts of the ipso and meta carbons shows a clear trend; they are shifted downfield as the substituent becomes more electron withdrawing (NMe_2 → OMe → H → CO_2Me). The trend for the para carbons can also be rationalized by the extent of deshielding (**1c** > **1b** > **1d** > **1a**). In such close proximity, it is mainly influenced by the electronegativity of the attached atom (O > N > C > H). For the same reason, chemical shifts for the ortho carbons (165.37−165.92 ppm) are primarily determined by the phosphinite oxygen atoms and thus are almost insensitive to the para substituent.

As expected, the IR spectrum of each cobalt dicarbonyl complex exhibits two strong bands in the 1900−2000 cm^{-1} region characteristic of CO ligands. Although the differences in wavenumbers for **1a−d** are small (Table 1), the CO bands consistently shift to higher frequencies (**1b** < **1c** < **1a** < **1d**) when the pincer ligand becomes less donating, which would result in less back-donation from cobalt to the CO π^* orbital. Complex **1e** has two CO bands with higher frequencies, suggesting that replacing the isopropyl groups with phenyl groups significantly reduces the pincer donor ability. As a further comparison, the *tert*-butyl derivative {2,6-$(^tBu_2PO)_2C_6H_3$}$Co(CO)_2$ (in CH_2Cl_2, 1969 and 1915 cm^{-1})[16] has CO bands similar in energy to those of **1a**. The phosphine-based PCP pincer complex {2,6-$(Ph_2PCH_2)_2C_6H_3$}$Co(CO)_2$ contains a more electron rich ligand in comparison to **1e**, as indicated by two lower energy CO bands at 1982 and 1929 cm^{-1} (in CH_2Cl_2).[18] Kirchner's {2,6-$(^iPr_2PNMe)_2C_6H_3$}$Co(CO)_2$ shows CO bands at 1963 and 1906 cm^{-1} (for a solid sample),[19] implying that in terms of electronic properties the bis(phosphinous amide)-based pincer ligand is comparable to a dimethylamino-substituted POCOP pincer ligand (i.e., ligand in **1b**).

The solid-state structures of **1a−e** were studied by X-ray crystallography (Figures 1−5), and key structural parameters are summarized in Table 2. On the basis of the geometry index τ calculated for each complex (0.1−0.4),[30] the coordination

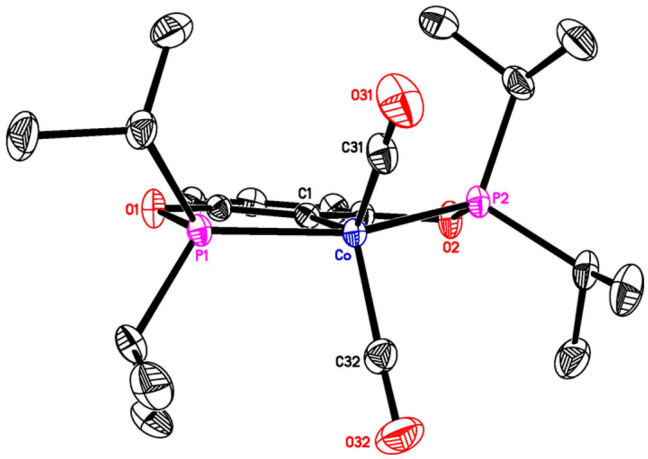

Figure 1. ORTEP drawing of {2,6-$(^iPr_2PO)_2C_6H_3$}$Co(CO)_2$ (**1a**) at the 50% probability level (hydrogen atoms omitted for clarity).

geometry is best described as distorted square pyramidal. Interestingly, there is very little variation with the Co−C_{ipso} bond lengths, regardless of the type of substituent introduced to the para position or the phosphorus donors. The Co−P bond lengths are, however, dependent on the size of the phosphorus substituents. In comparison to the isopropyl derivatives **1a−d** (2.1574−2.1697 Å) and the phenyl derivative **1e** (2.1451 and 2.1553 Å), the Co−P bonds of **1f** (2.2112 and 2.2119 Å) are significantly elongated, presumably due to the steric congestion imposed by the *tert*-butyl groups. The apical CO ligand forms a longer Co−C bond than does the basal CO ligand, typically by 0.03−0.05 Å. The apical C−O bond is slightly shorter than the basal C−O bond, with **1f** being the only exception. The P−Co−P and OC−Co−CO bond angles differ with a change of substituents, although there are no obvious trends. Of particular note is complex **1b**, which crystallizes as two independent molecules in the lattice (Figure 2). The nitrogen center of the NMe_2 group is pyramidal in one molecule ($\sum N$ = 344.9°, molecule A) while it is planar in the other ($\sum N$ = 359.9°, molecule B).

Catalytic Studies. We have previously shown that {2,6-$(^iPr_2PO)_2C_6H_3$}NiH catalyzes the hydrosilylation of aldehydes and ketones via carbonyl insertion into the Ni−H bond.[13d] We have also reported similar reactions catalyzed by *cis*-{2,6-$(^iPr_2PO)_2C_6H_3$}$Fe(PMe_3)_2H$.[31] Despite the similarities in ancillary ligands, our mechanistic studies including deuterium-labeling experiments suggest that, for the iron system, the hydride ligand does not directly participate in the catalytic cycle. Instead, it promotes the dissociation of the *trans*-PMe_3, thereby creating a Lewis acidic iron center for substrate binding or activation. However, DFT calculations performed by Wei and co-workers support a mechanism involving carbonyl insertion into the Fe−H bond.[32] We were thus curious to see if the cobalt carbonyl complexes reported here, which do not contain a metal−hydrogen bond, would also catalyze the hydrosilylation reactions. Additionally, we noted that, in comparison to other metal systems,[33] cobalt complexes had been relatively underexplored as catalysts for the hydrosilylation of carbonyl functionalities.[34]

The initial catalytic experiment was conducted at 50 °C in a sealed J. Young NMR tube charged with PhCHO, $(EtO)_3SiH$ (1.1 equiv), **1a** (1 mol % catalyst loading), hexamethylbenzene (internal standard), and C_6D_6. To our disappointment, no

DOI: 10.1021/acs.organomet.8b00273
Organometallics XXXX, XXX, XXX−XXX

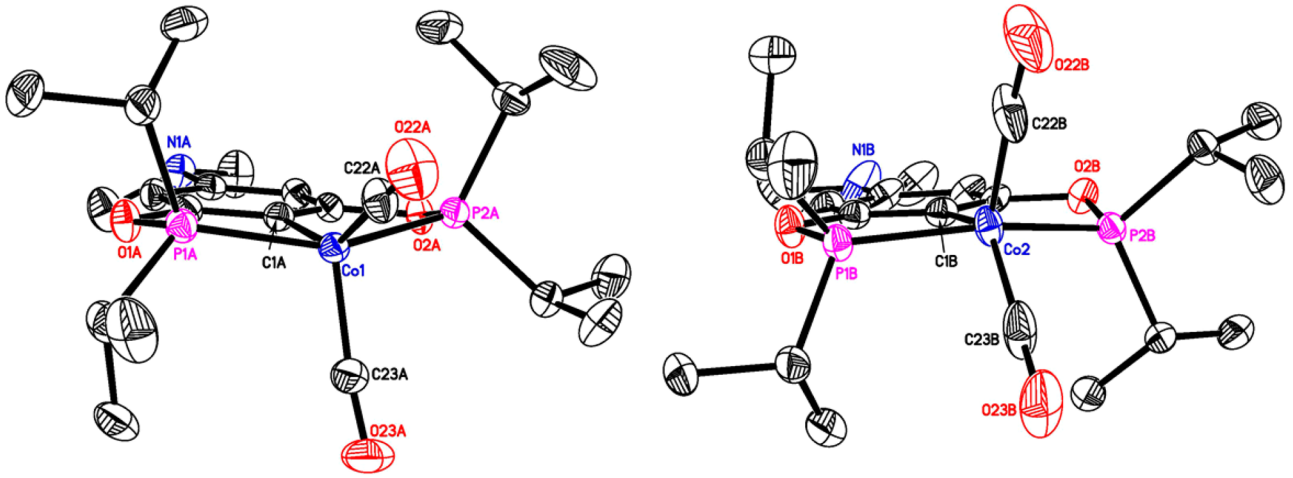

Figure 2. ORTEP drawings of $\{2,6\text{-}(^{i}Pr_2PO)_2\text{-}4\text{-}NMe_2\text{-}C_6H_2\}Co(CO)_2$ (**1b**) at the 50% probability level (hydrogen atoms omitted for clarity). Two independent molecules were found in the unit cell.

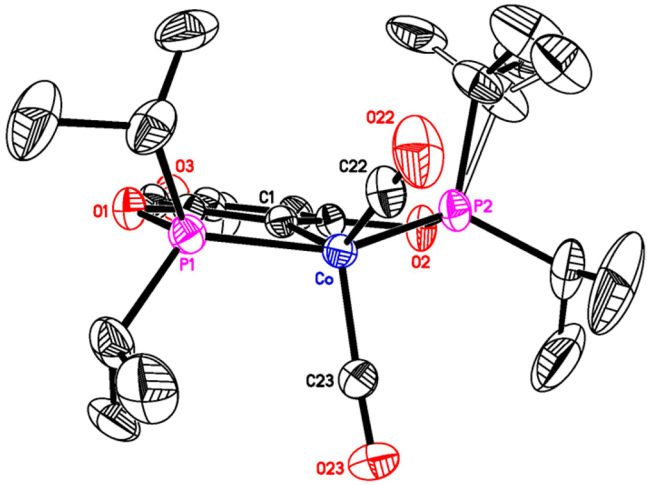

Figure 3. ORTEP drawing of $\{2,6\text{-}(^{i}Pr_2PO)_2\text{-}4\text{-}OMe\text{-}C_6H_2\}Co(CO)_2$ (**1c**) at the 50% probability level (hydrogen atoms omitted for clarity).

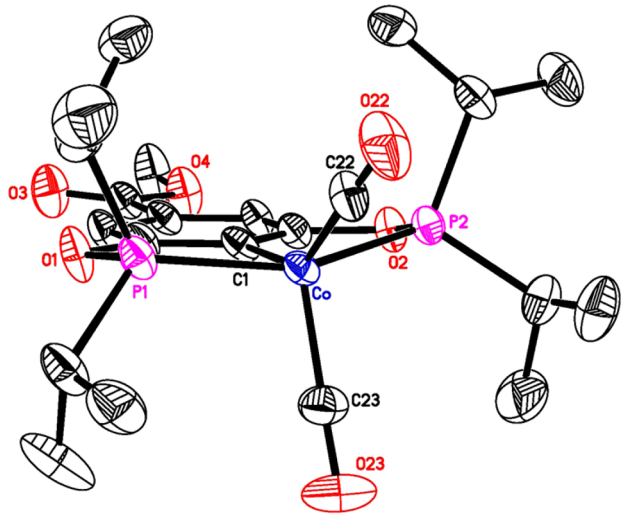

Figure 4. ORTEP drawing of $\{2,6\text{-}(^{i}Pr_2PO)_2\text{-}4\text{-}CO_2Me\text{-}C_6H_2\}Co(CO)_2$ (**1d**) at the 50% probability level (hydrogen atoms omitted for clarity).

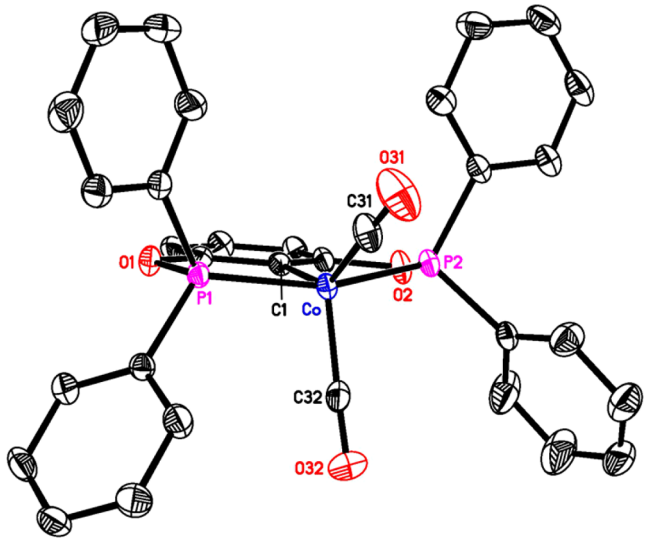

Figure 5. ORTEP drawing of $\{2,6\text{-}(Ph_2PO)_2C_6H_3\}Co(CO)_2$ (**1e**) at the 50% probability level (hydrogen atoms omitted for clarity).

hydrosilylation product was detected after 24 h (Table 3, entry 1). Increasing the temperature to 80 °C led to ~10% conversion of PhCHO to $(PhCH_2O)Si(OEt)_3$ (entry 2). The conversion could be increased by raising the temperature further to 100 °C (entry 3), although multiple hydrosilylation products started to emerge, likely due to alkoxide exchange on silicon to form $(PhCH_2O)_xSi(OEt)_{4-x}$ (x = 1−4). Considering that **1a** is an 18-electron complex, we turned our attention to strategies of removing CO to generate a vacant coordination site at the cobalt center. Addition of Me_3NO, which was previously used to abstract CO from iron carbonyl complexes,[35] failed to enhance the catalytic activity of **1a** (entry 4). Irradiation of the NMR tube with an array of four 365 nm UV-LEDs (performed at 23 °C) did improve the conversion to 87%; however, the combined yield for the hydrosilylation products was merely 15% with many photo-products difficult to characterize (entry 5). A significant improvement in the conversion and the yield was achieved when the NMR tube was connected to a Schlenk line filled with argon, in which case PhCHO was converted to $(PhCH_2O)Si(OEt)_3$ quantitatively (entry 6). Presumably, in

DOI: 10.1021/acs.organomet.8b00273
Organometallics XXXX, XXX, XXX−XXX

Table 2. Selected Crystallographic Data for the Cobalt Dicarbonyl Complexes

complex	R′	R	τ^c	Co−C_{ipso} (Å)	Co−P (Å)	Co−C_{ap}O (Å)[d]	C_{ap}−O (Å)	Co−C_{ba}O (Å)[d]	C_{ba}−O (Å)	P−Co−P (deg)	OC−Co−CO (deg)
1a	H	^{i}Pr	0.32	1.9885(10)	2.1660(3), 2.1668(3)	1.7838(12)	1.1432(15)	1.7564(12)	1.1527(15)	155.024(13)	109.20(6)
1b[a]	NMe_2	^{i}Pr	0.10	1.981(3)	2.1623(9), 2.1674(9)	1.797(3)	1.140(4)	1.745(3)	1.155(4)	151.68(4)	109.69(17)
			0.40	1.977(3)	2.1642(9), 2.1677(9)	1.776(4)	1.146(5)	1.747(4)	1.162(5)	155.51(4)	116.1(2)
1c	OMe	^{i}Pr	0.16	1.9865(19)	2.1574(6), 2.1618(6)	1.785(2)	1.146(3)	1.749(2)	1.149(3)	150.49(2)	110.39(11)
1d	CO_2Me	^{i}Pr	0.23	1.966(4)	2.1670(13), 2.1697(12)	1.792(5)	1.144(6)	1.747(5)	1.146(6)	153.44(5)	111.1(2)
1e	H	Ph	0.26	1.9737(15)	2.1451(4), 2.1553(4)	1.8046(17)	1.138(2)	1.7553(17)	1.149(2)	155.737(18)	113.88(8)
1f[b]	H	^{t}Bu	0.08	1.9776(16)	2.2112(5), 2.2119(5)	1.7962(18)	1.148(2)	1.7657(18)	1.104(2)	152.28(2)	105.96(8)

[a]Complex **1b** crystallizes as two independent molecules; hence, two different sets of data are provided here. [b]Data obtained from ref 16. [c]$\tau = (\beta - \alpha)/60$; β and α are the two greatest bond angles (in degrees) about the cobalt. [d]ap = apical; ba = basal.

Table 3. Hydrosilylation of PhCHO with $(EtO)_3SiH$ Catalyzed by 1a[a]

$$PhCHO + (EtO)_3SiH \xrightarrow[C_6D_6]{1\ mol\%\ \mathbf{1a}} (PhCH_2O)Si(OEt)_3$$

entry	conditions	conversion (%)[d]	yield (%)[d]
1	50 °C, 24 h, closed	0	0
2	80 °C, 24 h, closed	10	7
3	80 °C for 24 h followed by 100 °C for 24 h, closed	78	78[e]
4	50 °C, 1 mol % Me_3NO, 24 h, closed	0	0
5	23 °C, $h\nu$ (365 nm), 24 h, closed	87	15[e]
6	50 °C, 24 h, open to argon	>99	>99
7	50 °C, 24 h, open to CO[b]	0	0
8	23 °C, 24 h, open to argon[c]	12	10
9	23 °C, $h\nu$ (365 nm), 24 h, open to argon	94	42[e]

[a]General information: PhCHO (1.0 mmol), $(EtO)_3SiH$ (1.1 mmol), **1a** (0.010 mmol), and hexamethylbenzene (0.050 mmol, internal standard) mixed with 225 μL of C_6D_6 in a J. Young NMR tube. [b]The NMR tube was connected to a Schlenk line filled with CO. [c]2 mol % catalyst loading. [d]Determined by ^{1}H NMR. [e]Multiple products were present. The combined yield for $PhCH_2O$-containing products is shown here.

an open system, CO is allowed to escape from the reaction solution, thus forming an appreciable amount of the active species. Consistent with this hypothesis, when the Schlenk line was filled with CO (~1 atm), the hydrosilylation reaction was completely suppressed (entry 7). With the open system setup (under argon), attempts were made to carry out the catalytic reaction at room temperature. The results were unsatisfactory, even when the catalyst loading was increased to 2 mol % (entry 8). Evidently, the open system also helped promote aldehyde conversion under photochemical conditions (entry 9 vs entry 5), although the selectivity for the hydrosilylation products remained low.

A closer monitoring of the open-system reaction at 50 °C (Table 3, entry 6) showed that the hydrosilylation process needed only 10 h to complete. Replacing $(EtO)_3SiH$ with $PhSiH_3$ under the same conditions resulted in a slightly faster catalytic reaction, converting PhCHO to several $PhCH_2O$-containing products in 8 h. Ph_2SiH_2 also proved to be a viable silane to reduce PhCHO, albeit requiring 24 h to complete the hydrosilylation reaction. In contrast, Et_3SiH was completely ineffective; no hydrosilylation product was observed, even after 48 h.

To understand how different POCOP pincer ligands influence the catalytic activity, hydrosilylation of PhCHO with $(EtO)_3SiH$ catalyzed by other cobalt carbonyl complexes (**1b−e** and **2f**) was examined under the optimized conditions. As illustrated by the reaction profiles (Figure 6), all reactions including that with **1a** showed an induction period of 2−6 h. The hydrosilylation process was noticeably faster when **1b** or **1c** was employed as the catalyst. In fact, the catalytic performance of these cobalt pincer complexes is well correlated to the electronic properties of the para substituents with a decreasing order of activity: **1b** (R′ = NMe_2) > **1c** (R′ = OMe) > **1a** (R′ = H) > **1d** (R′ = CO_2Me). In comparison to **1a−d**, complex **1e** bears the far less electron rich POCOP pincer ligand $[2,6\text{-}(Ph_2PO)_2C_6H_3]^-$, as measured by the ν_{CO} values (Table 1). It was thus not surprising to see that **1e** was the least efficient catalyst. The *tert*-butyl derivative **2f** is already a 16-electron complex; however, like **1a−e**, it was catalytically

DOI: 10.1021/acs.organomet.8b00273
Organometallics XXXX, XXX, XXX−XXX

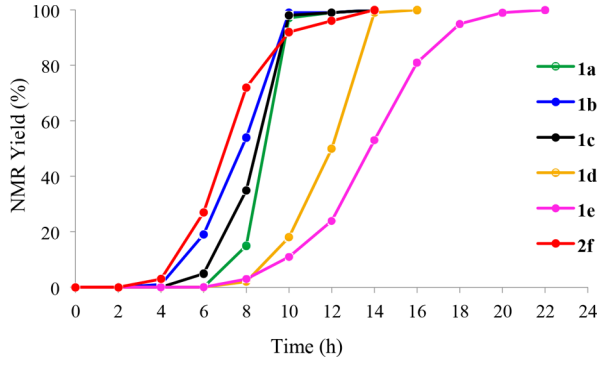

Figure 6. NMR yield of $PhCH_2OSi(OEt)_3$ as a function of time (reaction conditions: 1.0 mmol of PhCHO, 1.1 mmol of $(EtO)_3SiH$, 1 mol % catalyst, and 0.050 mmol of hexamethylbenzene mixed in 225 μL of C_6D_6, 50 °C, open to argon).

inactive at 50 °C when the reaction was conducted in a sealed NMR tube. Nevertheless, in an open system, hydrosilylation of PhCHO catalyzed by **2f** had the shortest induction period (Figure 6), although over a longer period of time **2f** was outperformed by **1a–c**.

The substrate scope of our catalytic system was studied using **1b** as the catalyst and THF as the solvent.[36] The reactions were performed in a flask connected to a Schlenk line filled with argon. The reduction products were isolated in the alcohol form following hydrolysis of the initial hydrosilylation products. As demonstrated in Table 4, benzaldehyde and

Table 4. Hydrosilylation of Aldehydes or Ketones Catalyzed by 1b[a]

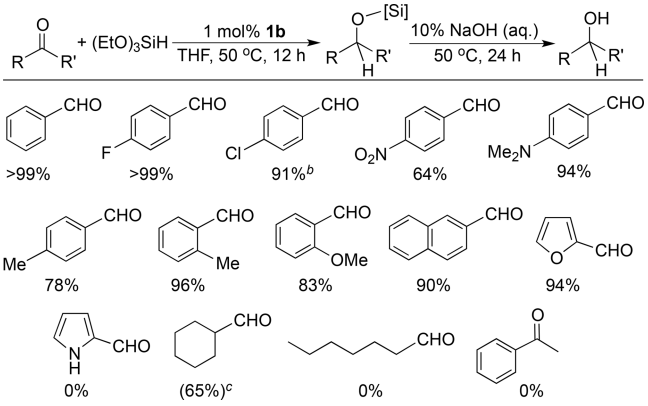

[a]Conditions: RCOR′ (2.0 mmol), $(EtO)_3SiH$ (2.2 mmol), and **1b** (0.020 mmol) mixed in 2 mL of THF, 50 °C, open to argon. Values given are the isolated yields for the alcohol products. [b]4.4 mmol of $(EtO)_3SiH$ was used. [c]Reaction time was increased to 24 h and the value given in parenthesis is for NMR conversion.

substituted benzaldehydes reacted smoothly to afford the corresponding alcohols in good yields, and compatible functional groups included F, Cl, NO_2, NMe_2, and OMe. For reasons unclear to us, the reaction of 4-chlorobenzaldehyde needed 2.2 equiv of $(EtO)_3SiH$ to reach completion. The catalytic protocol was amenable to other aromatic aldehydes such as 2-naphthaldehyde and 2-furaldehyde but was problematic with pyrrole-2-carboxaldehyde. Hydrosilylation of aliphatic aldehydes such as cyclohexanecarboxaldehyde was shown to be possible but slow (65% conversion over 24 h). In contrast, heptanal was not a viable substrate for the hydrosilylation reaction. Similarly, the hydrosilylation of acetophenone failed to take place under the catalytic conditions.

CO Dissociation from the Dicarbonyl Complexes. As an important piece of mechanistic information, CO dissociation from **1a–e** is a kinetically favorable but thermodynamically uphill process. Even at room temperature, these cobalt dicarbonyl complexes (dissolved in C_6D_6) underwent ligand exchange with ^{13}CO (1 atm) within hours. Unlike {2,6-(^{t}Bu$_2$PO)$_2$C$_6$H$_3$}Co(CO)$_2$ (**1f**), which at room temperature under vacuum was partially converted to {2,6-(^{t}Bu$_2$PO)$_2$C$_6$H$_3$}Co(CO) (**2f**),[16] none of the isopropyl and phenyl derivatives lost CO after a prolonged period of evacuation. To study their stability at higher temperatures, **1b** was chosen as a representative compound. At 70 °C (heated by an oil bath) under dynamic vacuum, the solid sample gradually changed color from orange to dark brown. After 3 days, the residue was dissolved in C_6D_6 for NMR analysis, which indicated significant decomposition of **1b** (~40% based on $^{31}P\{^1H\}$ NMR). However, in a closed system, **1b** proved to be incredibly robust. A toluene-d_8 solution of **1b** sealed in a J. Young NMR tube did not change color until the temperature was raised to above 100 °C. Interestingly, the ^1H NMR spectrum of the sample heated at 200 °C for 24 h without disturbing the headspace showed a new species along with unreacted **1b** (Figure 7). Shaking the NMR tube led to an instantaneous color change back to orange, and the NMR spectrum confirmed that **1b** was fully recovered. This process could be repeated with the same sample multiple times without noticeable decomposition of **1b**. Isolation and full characterization of the new species were not possible. Given the reversibility demonstrated in Figure 7 and the precedents of CO loss from five-coordinate Co(I) dicarbonyl complexes,[16,37] we propose that the darkening of the solution is due to the formation of the monocarbonyl complex {2,6-(^{i}Pr$_2$PO)$_2$-4-NMe$_2$-C$_6$H$_2$}Co(CO) (**2b**).

The CO ligands of the cobalt dicarbonyl complexes can be displaced if another coordinating ligand is present. This was demonstrated by the reaction of **1a** with *tert*-butyl isocyanide (Scheme 1). As one might have anticipated, the ligand substitution process became more favorable with an increase in temperature or the amount of *tert*-butyl isocyanide used. The conversions of **1a** were generally higher in an open system than in a closed system. The bis(isocyanide) complex **4a** was isolated in pure form by performing the substitution reaction at 80 °C and removing the decomposition products with cold methanol. Stopping the substitution process at the mono(isocyanide) stage was attempted under various conditions but with no success. To strike a balance between promoting step **1a** → **3a** and minimizing step **3a** → **4a**, **1a** was treated with 6 equiv of *tert*-butyl isocyanide at 50 °C for 24 h. The isolated material was identified as a 4:1 mixture of **3a** and **4a**, representing our best effort to enrich **3a**.

A few single crystals of **3a** were obtained by keeping a pentane solution of the **3a**/**4a** mixture at −30 °C. X-ray crystallography revealed a distorted-square-pyramidal geometry at cobalt with a τ value of 0.13. As shown in Figure 8, the isocyanide ligand occupies a basal site, whereas CO resides at the apical position. This result does not necessarily mean that the isocyanide ligand displaces the basal CO of **1a**. The NMR data of **1a** and **4a** (vide infra) suggest that, *in solution*, the two CO ligands and the two *tert*-butyl isocyanide ligands are equivalent, respectively. Likewise, in solution, the CO and the *tert*-butyl isocyanide of **3a** are likely to exchange sites rapidly.

DOI: 10.1021/acs.organomet.8b00273
Organometallics XXXX, XXX, XXX–XXX

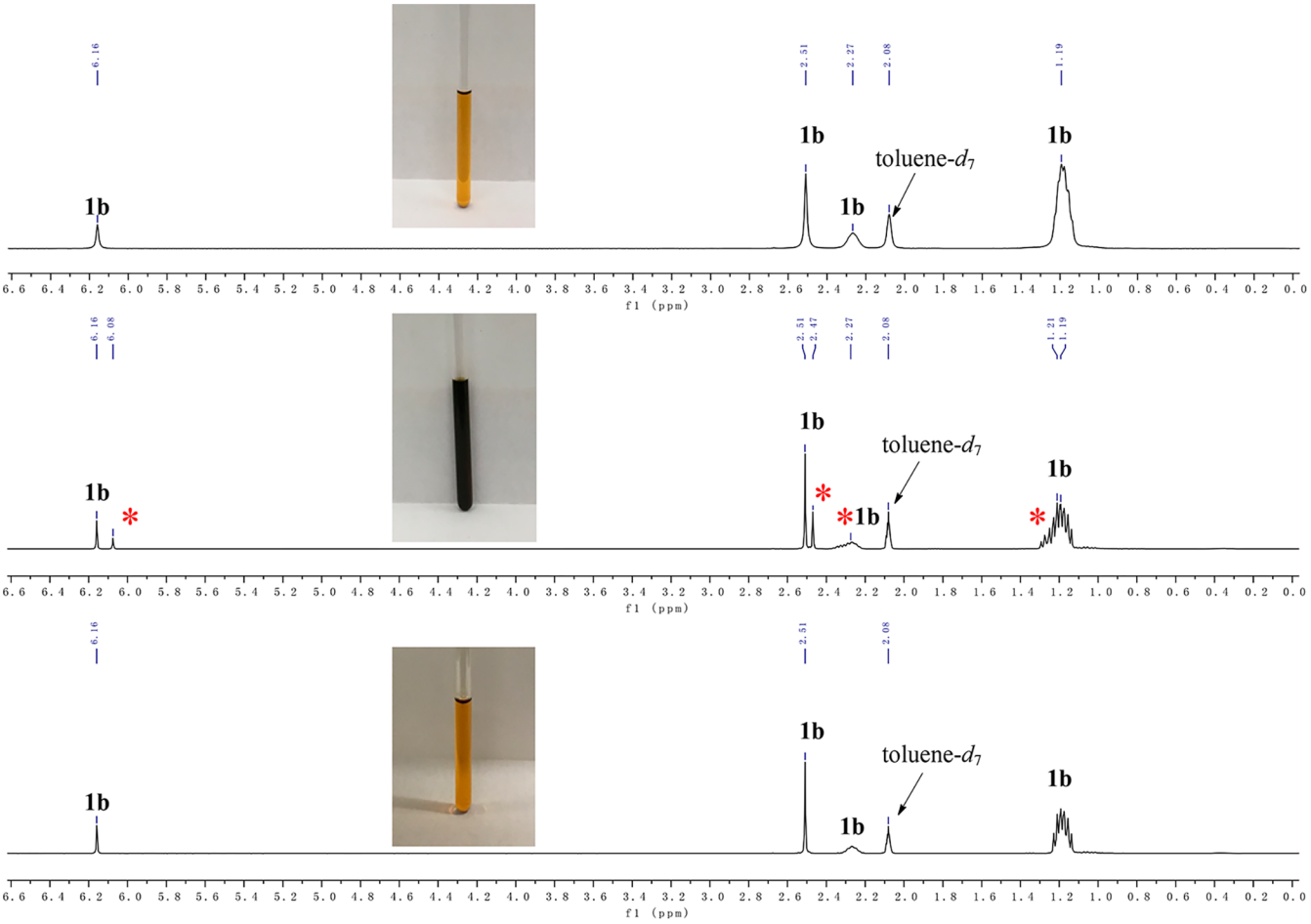

Figure 7. Thermal stability of **1b** in a closed system: (A) ^{1}H NMR spectrum of **1b** (in toluene-d_8) at 23 °C; (B) ^{1}H NMR spectrum of **1b** after being heated at 200 °C for 24 h without disturbing the headspace (asterisks designate a new species); (C) ^{1}H NMR spectrum of **1b** recovered from sample (B) upon shaking the NMR tube.

Scheme 1. Reactions of 1a with *tert*-Butyl Isocyanide

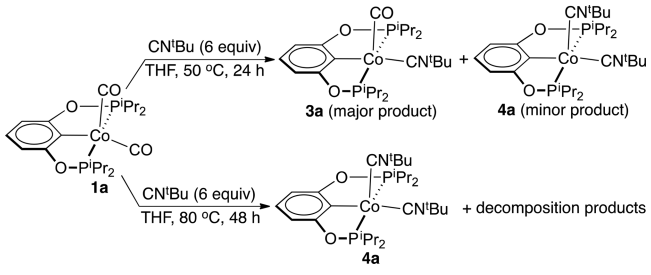

In comparison to the dicarbonyl complex **1a**, the Co−C_{ipso} and Co−P bonds of **3a** are contracted by 0.02 Å, presumably to compensate for the longer Co−C bond formed with the isocyanide ligand (1.8205(18) Å vs 1.7564(12) Å for the Co−C_{ba}O bond in **1a**). The P−Co−P bond angle of **3a** (145.28(2)°) is much smaller than that of **1a** (155.024(13)°). On the other hand, the bond metrics for the apical CO ligand are quite similar in these two complexes.

The solid-state structure of **4a** (Figure 9) illustrated that further substitution of CO for isocyanide did not significantly alter the coordination geometry (τ = 0.07) and Co−C_{ipso} and Co−P bond distances. A notable change is the isocyanide ligand at the basal site, which deviates greatly from linearity with a C−N−C bond angle of 143.76(12)°. In contrast, the C−N−C bond angle in **3a** (176.47(19)°) and that of the apical isocyanide in **4a** (175.51(13)°) are close to linear. The related complex {2,6-(^{i}Pr$_2$PNMe)$_2$C$_6$H$_3$}Co(CN^{t}Bu)$_2$ was also reported to have one bent isocyanide and one linear isocyanide.[38] This phenomenon has often been explained by invoking two different structures of isocyanide complexes, as depicted in Figure 10.[39] The bent structure (B) would require sufficient back-donation from the metal to the isocyanide π^* orbital. Consistent with this bonding picture, the Co−C bond in **4a** formed by the bent isocyanide is 0.04 Å shorter than the analogous bond in **3a** formed by the linear isocyanide, and the corresponding C≡N bond in **4a** is 0.03 Å longer than that in **3a**.

While the crystal structure of **4a** showed two different types of isocyanide ligands, NMR spectra of **4a** (in C_6D_6) suggested that the isocyanide ligands are equivalent. More specifically, only one multiplet (172.69 ppm) was observed for the CN resonance and one singlet was located for each of the $C(CH_3)_3$, $C(CH_3)_3$, and $C(CH_3)_3$ resonances. Additionally, only one $CH(CH_3)_2$ resonance was found for **4a**, further implying that the molecule has C_{2v} symmetry. The presence of both CO and an isocyanide ligand in **3a** was supported by $^{13}C\{^1H\}$ spectroscopy (for a sample dissolved in C_6D_6), which revealed a multiplet at 208.33 ppm attributed to the CO resonance and another multiplet at 163.20 ppm assigned to the CN^{t}Bu resonance.

DOI: 10.1021/acs.organomet.8b00273
Organometallics XXXX, XXX, XXX−XXX

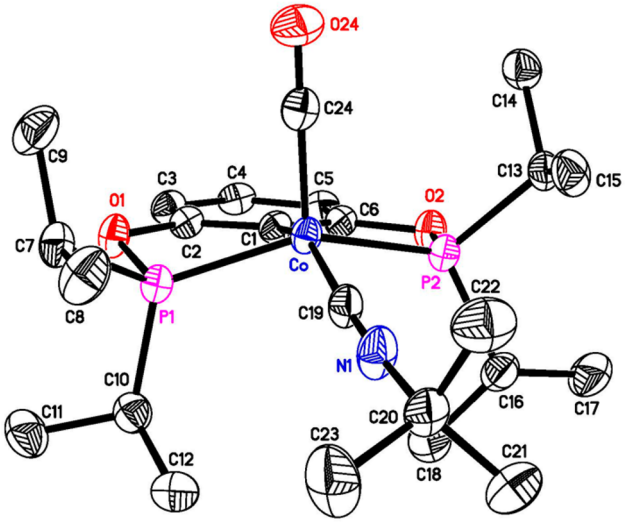

Figure 8. ORTEP drawing of {2,6-(^{i}Pr$_2$PO)$_2$C$_6$H$_3$}Co(CN^{t}Bu)(CO) (**3a**) at the 50% probability level (hydrogen atoms omitted for clarity). Selected bond lengths (Å) and angles (deg): Co−C(1) 1.9646(16), Co−C(19) 1.8205(18), Co−C(24) 1.7852(19), Co−P(1) 2.1469(5), Co−P(2) 2.1439(5), C(19)−N(1) 1.164(2), C(24)−O(24) 1.151(2); C(1)−Co−C(19) 152.83(8), C(1)−Co−C(24) 104.14(7), C(19)−Co−C(24) 102.97(8), C(19)−N(1)−C(20) 176.47(19), P(1)−Co−P(2) 145.28(2).

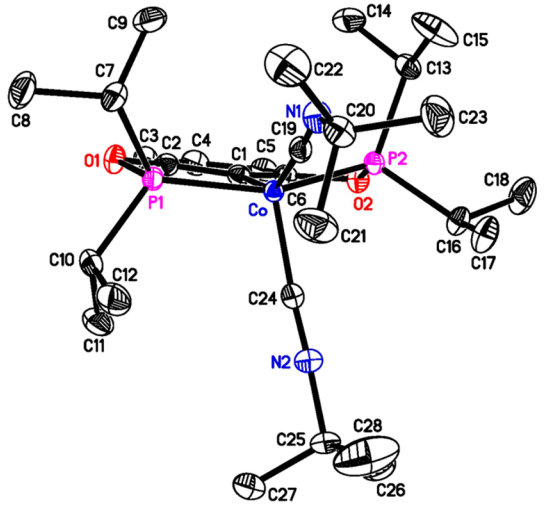

Figure 9. ORTEP drawing of {2,6-(^{i}Pr$_2$PO)$_2$C$_6$H$_3$}Co(CN^{t}Bu)$_2$ (**4a**) at the 50% probability level (hydrogen atoms omitted for clarity). Selected bond lengths (Å) and angles (deg): Co−C(1) 1.9620(11), Co−C(19) 1.7838(12), Co−C(24) 1.8674(12), Co−P(1) 2.1379(3), Co−P(2) 2.1303(3), C(19)−N(1) 1.1901(16), C(24)−N(2) 1.1642(16); C(1)−Co−C(19) 148.22(5), C(1)−Co−C(24) 106.38(5), C(19)−Co−C(24) 105.38(5), C(19)−N(1)−C(20) 143.76(12), C(24)−N(2)−C(25) 175.51(13), P(1)−Co−P(2) 152.637(14).

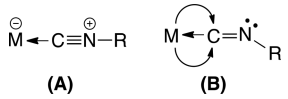

Figure 10. Linear and bent structures of isocyanide complexes.

Complex **4a** was tested as a catalyst (1 mol % loading) for the hydrosilylation of PhCHO with (EtO)$_3$SiH performed at 50 °C in C$_6$D$_6$. After 24 h, 47% of PhCHO was converted, as judged by ^{1}H NMR spectroscopy, resulting in (PhCH$_2$O)$_x$Si(OEt)$_{4-x}$ with a combined yield of 42%. This result suggests that **4a** is a less effective catalyst than **1a** (cf. Table 3, entry 6). However, with **4a**, the catalytic reaction can be carried out in a closed system.

Mechanistic Considerations. The CO dissociation or substitution reactions described above prompted us to examine the possibility that, under the catalytic conditions, CO could be displaced by either the aldehyde or (EtO)$_3$SiH. Thus, a mixture of PhCHO and **1b** (with a ratio of 100:1) in C$_6$D$_6$ was heated at 50 °C and monitored by ^{1}H and ^{31}P{^{1}H} NMR spectroscopy. After 24 h, no new species could be detected, regardless of whether the mixture was kept in a closed or an open system. Similarly, a sealed J. Young NMR tube containing a 110:1 mixture of (EtO)$_3$SiH and **1b** in C$_6$D$_6$ was heated at 50 °C for 24 h but did not yield any new product. However, when the NMR tube was connected to a Schlenk line filled with argon, **1b** started to decompose (~25% over 24 h). These results suggest that, unlike *tert*-butyl isocyanide, neither PhCHO nor (EtO)$_3$SiH is capable of competing with CO for a vacant coordination site at cobalt. Nevertheless, we cannot rule out the scenario that the PhCHO- or (EtO)$_3$SiH-bound complex was present in a small amount beyond the NMR detection limit, yet such an intermediate could be highly catalytically active.

To discern which reactant initiated catalyst activation, we mixed **1b** with one reactant first and let the mixture "age" for 24 h under the catalytic conditions, followed by the addition of the other reactant (Scheme 2). The time required to fully

Scheme 2. Catalytic Hydrosilylation of PhCHO with Different Addition Sequences

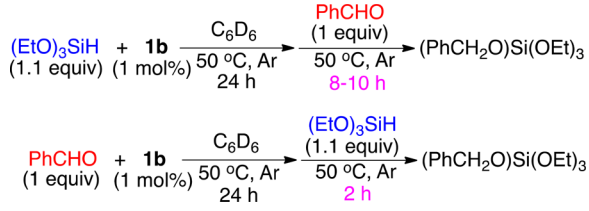

reduce PhCHO was found to depend on the addition sequence. The silane-first procedure needed 8−10 h to reach completion, which is similar to the standard protocol that initially mixes both PhCHO and (EtO)$_3$SiH with catalyst **1b** (Figure 6). In contrast, the aldehyde-first procedure shortened the reaction time to 2 h. With the catalyst preactivated by PhCHO, the hydrosilylation step could be carried out in a closed system without sacrificing the catalytic efficiency. We also noted that, once the hydrosilylation reaction was complete, replenishing PhCHO and (EtO)$_3$SiH reinitiated the catalytic reaction, which took only 2 h to fully reduce PhCHO. This process was repeated one more time with >99% conversion achieved in 2 h, giving a combined turnover number of 300.

A sigmoidal reaction profile, like those shown in Figure 6, is often suspected as a reaction catalyzed by nanoparticulates, although it can also mean a slow conversion of the catalyst precursor to an active species.[40] A mercury test was negative; **1b**-catalyzed hydrosilylation of PhCHO with (EtO)$_3$SiH was unaffected by the addition of Hg(0) (100 equiv with respect to **1b**). PPh$_3$ was also employed as a poisoning reagent. Adding 5 mol % of PPh$_3$ (i.e., PPh$_3$:**1b** = 5:1) to the reaction mixture did

DOI: 10.1021/acs.organomet.8b00273
Organometallics XXXX, XXX, XXX−XXX

not suppress the catalytic reaction but prolonged the reaction time from 10 to 18 h. It is reasonable to assume that PPh_3 can facilitate CO dissociation but at the same time block the coordination site needed for hydrosilylation. On the basis of the mercury test and the PPh_3 experiment, we favor the notion that our catalytic system is homogeneous in nature.

At this point, we are certain that the catalytic hydrosilylation reactions begin with CO dissociation from the cobalt dicarbonyl complexes. This is consistent with the observation that CO inhibited the catalytic reactions. Understandably, the CO dissociation step is more favorable at higher temperatures both kinetically and thermodynamically. Isocyanide ligands displace CO to a great extent at 23−80 °C, and aldehydes may also displace CO in the same temperature range, albeit to a much lesser extent. The thermodynamics can be improved by performing the reactions in an open system, which allows the gaseous CO to escape from the reaction mixture. What we are unsure about are the mechanistic details after CO dissociation. The fact that **2f** is an inactive catalyst at 50 °C in a closed system may suggest the necessity of removing the second CO ligand, although it may be only required for the bulky {2,6-(^{t}Bu$_2$PO)$_2$C$_6$H$_3$}Co pincer system. It is also possible that the hydrosilylation reactions are catalyzed by species that decompose from the cobalt POCOP pincer complexes. Efforts are underway to further elucidate the mechanistic details, and the results will be reported in due course.

CONCLUSIONS

In this work, we have developed a new synthetic strategy for cobalt pincer complexes that involves C−H bond activation of POCOP pincer ligands with $Co_2(CO)_8$. This new method has allowed us to access a variety of cobalt POCOP pincer complexes, especially those with cleavable P−O bonds and rigid backbone, which are otherwise difficult to synthesize. We have also demonstrated that the cobalt dicarbonyl complexes catalyze the hydrosilylation of aldehydes with $(EtO)_3SiH$ at elevated temperatures (≥100 °C) in a closed system or at 50 °C in an open system. Our mechanistic investigation has suggested that CO dissociation is kinetically favorable even at room temperature but is thermodynamically uphill. From reaction profiles, we have observed an induction period, likely due to a slow dissociation of CO to yield a catalytically active species. The reaction time can be significantly shortened when the catalyst is preactivated by an aldehyde or, after the catalytic reaction is complete, more reagents are added to the catalytic mixture to reinitiate the hydrosilylation reaction. Furthermore, we have shown that the catalytic reactions are not poisoned by a large excess of Hg(0) and PPh_3 but are slowed down by the latter, indicating a homogeneous catalytic system.

EXPERIMENTAL SECTION

General Comments. Unless otherwise noted, all organometallic compounds were prepared and handled under an argon atmosphere using standard glovebox and Schlenk techniques. Dry and oxygen-free solvents (THF, pentane, toluene, and diethyl ether) were collected from an Innovative Technology solvent purification system and used throughout the experiments. Methanol was degassed by bubbling argon through it for 30 min and then dried over 4 Å molecular sieves before use. Dichloromethane-d_2 (99.5% D) was purchased from Cambridge Isotope Laboratories, Inc. and used without further purification. Benzene-d_6 (99.5% D) was dried over Na-benzophenone and distilled under an argon atmosphere. All aldehydes were freshly distilled or purified by recrystallization. 1,3-(^{i}Pr$_2$PO)$_2$C$_6$H$_4$,[9i] 1,3-(Ph$_2$PO)$_2$C$_6$H$_4$,[41] 1,3-(^{i}Pr$_2$PO)$_2$-5-OMe-C$_6$H$_3$,[13i] 1,3-(^{i}Pr$_2$PO)$_2$-5-CO_2Me-C$_6$H$_3$,[13i] 1,3-(^{t}Bu$_2$PO)$_2$C$_6$H$_4$,[9a] and 5-dimethylamine resorcinol[9f] were prepared as described in the literature. Chemical shift values for ^{1}H and ^{13}C{^{1}H} NMR spectra were referenced internally to the residual solvent resonances. ^{31}P{^{1}H} NMR spectra were referenced externally to 85% H_3PO_4 (0 ppm). Infrared spectra were recorded on a Thermo Scientific Nicolet 6700 FT-IR spectrometer or PerkinElmer Spectrum Two FT-IR spectrometer equipped with a smart orbit diamond attenuated total reflectance (ATR) accessory.

Synthesis of {2,6-(^{i}Pr$_2$PO)$_2$C$_6$H$_3$}Co(CO)$_2$ (1a). In a glovebox, 1,3-(^{i}Pr$_2$PO)$_2$C$_6$H$_4$ (0.80 g, 2.34 mmol) dissolved in 20 mL of toluene was added dropwise to a Schlenk flask containing a solution of $Co_2(CO)_8$ (0.32 g, 0.94 mmol) in 15 mL of toluene. The flask was taken outside of the glovebox, connected to a Schlenk line, and heated with stirring at 110 °C for 24 h, during which time the reaction mixture changed gradually from dark red to orange-yellow. The volatiles were removed under reduced pressure, and the yellowish oily residue was treated with 40 mL of pentane and filtered into another Schlenk flask via a cannula. The filtrate was concentrated under vacuum to give a yellow oily residue, which was triturated with chilled (0 °C) methanol (1.5 mL × 3). The resulting solid was dried under vacuum to afford the product as a yellow solid (0.65 g, 76% yield). ^{1}H NMR (400 MHz, C$_6$D$_6$, δ): 6.82−6.78 (m, Ar*H*, 1H), 6.71−6.69 (m, Ar*H*, 2H), 2.28−2.16 (m, C*H*(CH$_3$)$_2$, 4H), 1.17−1.08 (m, CH(C*H*$_3$)$_2$, 24H). ^{1}H NMR (400 MHz, CD$_2$Cl$_2$, δ): 6.71 (t, J_{H-H} = 7.8 Hz, Ar*H*, 1H), 6.40 (d, J_{H-H} = 7.8 Hz, Ar*H*, 2H), 2.58−2.44 (m, C*H*(CH$_3$)$_2$, 4H), 1.30−1.23 (m, CH(C*H*$_3$)$_2$, 24H). ^{13}C{^{1}H} NMR (101 MHz, C$_6$D$_6$, δ): 205.71 (t, J_{P-C} = 15.4 Hz, *C*O), 165.99 (t, J_{P-C} = 8.0 Hz, Ar*C*), 137.89 (t, J_{P-C} = 21.4 Hz, Ar*C*), 125.37 (s, Ar*C*), 104.63 (t, J_{P-C} = 6.5 Hz, Ar*C*), 32.49 (t, J_{P-C} = 13.1 Hz, CH(CH$_3$)$_2$), 16.92 (t, J_{P-C} = 2.0 Hz, CH(*C*H$_3$)$_2$), 16.75 (s, CH(*C*H$_3$)$_2$). ^{13}C{^{1}H} NMR (101 MHz, CD$_2$Cl$_2$, δ): 205.40 (m, *C*O), 165.70 (t, J_{P-C} = 7.1 Hz, Ar*C*), 138.13 (t, J_{P-C} = 21.2 Hz, Ar*C*), 124.74 (s, Ar*C*), 104.09 (t, J_{P-C} = 6.1 Hz, Ar*C*), 32.68 (t, J_{P-C} = 13.1 Hz, *C*H(CH$_3$)$_2$), 17.07 (s, CH(*C*H$_3$)$_2$), 16.87 (s, CH(*C*H$_3$)$_2$). ^{31}P{^{1}H} NMR (202 MHz, C$_6$D$_6$, δ): 228.21 (s). ^{31}P{^{1}H} NMR (202 MHz, CD$_2$Cl$_2$, δ): 228.63 (s). Selected ATR-IR data (solid, cm^{-1}): 1966 (s, ν_{CO}), 1912 (s, ν_{CO}). Anal. Calcd for C$_{20}$H$_{31}$O$_4$P$_2$Co: C, 52.64; H, 6.85. Found: C, 52.84; H, 6.97.

Synthesis of 1,3-(^{i}Pr$_2$PO)$_2$-5-NMe$_2$-C$_6$H$_3$. In a glovebox, ^{i}Pr$_2$PCl (4.98 mL, 31.3 mmol) dissolved in 20 mL of THF was added dropwise to a Schlenk flask containing a well-stirred mixture of 5-dimethylamine resorcinol (2.18 g, 14.2 mmol), Et$_3$N (4.96 mL, 35.6 mmol), and 25 mL of THF. The reaction mixture was stirred at room temperature for 24 h, at which point a voluminous amount of white precipitate formed. The volatiles were removed under reduced pressure, and the yellow oily residue was washed with pentane (60 mL × 3) and filtered into another Schlenk flask via a cannula. The combined pentane filtrates were concentrated under vacuum to afford the product as a yellow oil (5.35 g, 98% yield). ^{1}H NMR (400 MHz, C$_6$D$_6$, δ): 6.83 (quint, $^4J_{P-H}$ = $^4J_{H-H}$ = 2.0 Hz, Ar*H*, 1H), 6.33 (br, Ar*H*, 2H), 2.55 (s, N(CH$_3$)$_2$, 6H), 1.77 (sept of d, J_{H-H} = 6.8 Hz, J_{P-H} = 2.8 Hz, C*H*(CH$_3$)$_2$, 4H), 1.15 (dd, J_{P-H} = 10.4 Hz, J_{H-H} = 6.8 Hz, CH(C*H*$_3$)$_2$, 12H), 1.01 (dd, J_{P-H} = 15.6 Hz, J_{H-H} = 6.8 Hz, CH(C*H*$_3$)$_2$, 12H). ^{13}C{^{1}H} NMR (101 MHz, C$_6$D$_6$, δ): 161.51 (d, J_{P-C} = 9.1 Hz, Ar*C*), 152.54 (s, Ar*C*), 98.00 (t, J_{P-C} = 13.1 Hz, Ar*C*), 97.22 (d, J_{P-C} = 11.1 Hz, Ar*C*), 40.26 (s, N(CH$_3$)$_2$), 28.64 (d, J_{P-C} = 18.2 Hz, CH(CH$_3$)$_2$), 18.07 (d, J_{P-C} = 20.2 Hz, CH(CH$_3$)$_2$), 17.31 (d, J_{P-C} = 9.1 Hz, CH(CH$_3$)$_2$). ^{31}P{^{1}H} NMR (162 MHz, C$_6$D$_6$, δ): 143.62 (s).

Synthesis of {2,6-(^{i}Pr$_2$PO)$_2$-4-NMe$_2$-C$_6$H$_2$}Co(CO)$_2$ (1b). This compound was prepared in 71% yield (as an orange solid) by a procedure similar to that used for **1a**. ^{1}H NMR (400 MHz, C$_6$D$_6$, δ): 6.30 (s, Ar*H*, 2H), 2.52 (s, N(C*H*$_3$)$_2$, 6H), 2.32−2.24 (m, C*H*(CH$_3$)$_2$, 4H), 1.24−1.15 (m, CH(C*H*$_3$)$_2$, 24H). ^{1}H NMR (400 MHz, CD$_2$Cl$_2$, δ): 5.95 (s, Ar*H*, 2H), 2.82 (s, N(C*H*$_3$)$_2$, 6H), 2.52−2.44 (m, C*H*(CH$_3$)$_2$, 4H), 1.43−1.08 (m, CH(C*H*$_3$)$_2$, 24H). ^{13}C{^{1}H} NMR (101 MHz, C$_6$D$_6$, δ): 206.30 (m, *C*O), 166.34 (t, J_{P-C} = 8.1 Hz, Ar*C*), 151.19 (s, Ar*C*), 121.99 (t, J_{P-C} = 22.2 Hz, Ar*C*), 91.53 (t, J_{P-C} = 7.1 Hz, Ar*C*), 40.94 (s, N(CH$_3$)$_2$), 32.43 (t, J_{P-C} = 12.1 Hz, CH(CH$_3$)$_2$), 16.99 (br, CH(CH$_3$)$_2$), 16.81 (s, CH(CH$_3$)$_2$). ^{13}C{^{1}H} NMR (101

DOI: 10.1021/acs.organomet.8b00273
Organometallics XXXX, XXX, XXX−XXX

MHz, CD_2Cl_2, δ): 205.95 (m, CO), 165.92 (t, J_{P-C} = 8.1 Hz, ArC), 150.88 (s, ArC), 121.94 (m, ArC), 90.77 (t, J_{P-C} = 7.0 Hz, ArC), 41.31 (s, $N(CH_3)_2$), 32.56 (t, J_{P-C} = 13.0 Hz, $CH(CH_3)_2$), 17.07 (t, J_{P-C} = 2.2 Hz, $CH(CH_3)_2$), 16.87 (s, $CH(CH_3)_2$). $^{31}P\{^1H\}$ NMR (162 MHz, C_6D_6, δ): 227.87 (s). $^{31}P\{^1H\}$ NMR (162 MHz, CD_2Cl_2, δ): 228.28 (s). Selected ATR-IR data (solid, cm^{-1}): 1965 (s, ν_{CO}), 1906 (s, ν_{CO}). Anal. Calcd for $C_{22}H_{36}NO_4P_2Co$: C, 52.91; H, 7.27. Found: C, 52.66; H, 7.34.

Synthesis of {2,6-(^{i}Pr$_2$PO)$_2$-4-OMe-C$_6$H$_2$}Co(CO)$_2$ (1c). This compound was prepared in 86% yield (as a yellow solid) by a procedure similar to that used for **1a**. ^1H NMR (400 MHz, CD_2Cl_2, δ): 6.13 (s, Ar*H*, 2H), 3.71 (s, OCH_3, 3H), 2.70−2.41 (m, $CH(CH_3)_2$, 4H), 1.76−0.99 (m, $CH(CH_3)_2$, 24H). ^1H NMR (400 MHz, C_6D_6, δ): 6.48 (s, Ar*H*, 2H), 3.32 (s, OCH_3, 3H), 2.32−2.17 (m, $CH(CH_3)_2$, 4H), 1.27−1.03 (m, $CH(CH_3)_2$, 24H). $^{13}C\{^1H\}$ NMR (101 MHz, CD_2Cl_2, δ): 205.57 (t, J_{P-C} = 13.1 Hz, CO), 165.37 (t, J_{P-C} = 8.1 Hz, ArC), 159.41 (s, ArC), 126.64 (t, J_{P-C} = 22.2 Hz, ArC), 91.63 (t, J_{P-C} = 7.1 Hz, ArC), 55.79 (s, OCH_3), 32.71 (t, J_{P-C} = 13.1 Hz, $CH(CH_3)_2$), 17.12 (br, $CH(CH_3)_2$), 16.94 (s, $CH(CH_3)_2$). $^{31}P\{^1H\}$ NMR (162 MHz, C_6D_6, δ): 229.31 (s). $^{31}P\{^1H\}$ NMR (162 MHz, CD_2Cl_2, δ): 229.61 (s). Selected ATR-IR data (solid, cm^{-1}): 1965 (s, ν_{CO}), 1908 (s, ν_{CO}). Anal. Calcd for $C_{21}H_{33}O_5P_2Co$: C, 51.86; H, 6.84. Found: C, 52.11; H, 6.92.

Synthesis of {2,6-(^{i}Pr$_2$PO)$_2$-4-CO$_2$Me-C$_6$H$_2$}Co(CO)$_2$ (1d). This compound was prepared in 84% yield (as a yellow solid) by a procedure similar to that used for **1a**. ^1H NMR (400 MHz, CD_2Cl_2, δ): 7.04 (s, Ar*H*, 2H), 3.80 (s, CO_2CH_3, 3H), 2.59−2.48 (m, $CH(CH_3)_2$, 4H), 1.31−1.23 (m, $CH(CH_3)_2$, 24H). $^{13}C\{^1H\}$ NMR (101 MHz, CD_2Cl_2, δ): 204.63 (t, J_{P-C} = 14.1 Hz, CO), 167.39 (s, CO_2CH_3), 165.52 (t, J_{P-C} = 8.1 Hz, ArC), 149.57 (t, J_{P-C} = 21.2 Hz, ArC), 127.08 (s, ArC), 104.89 (t, J_{P-C} = 6.1 Hz, ArC), 51.95 (s, CO_2CH_3), 32.77 (t, J_{P-C} = 13.1 Hz, $CH(CH_3)_2$), 17.01 (br, $CH(CH_3)_2$), 16.83 (s, $CH(CH_3)_2$). $^{31}P\{^1H\}$ NMR (162 MHz, CD_2Cl_2, δ): 229.45 (s). Selected ATR-IR data (solid, cm^{-1}): 1975 (s, ν_{CO}), 1919 (s, ν_{CO}), 1708 ($\nu_{C=O}$). Anal. Calcd for $C_{22}H_{33}O_6P_2Co$: C, 51.37; H, 6.47. Found: C, 51.82; H, 6.48.

Synthesis of {2,6-(Ph$_2$PO)$_2$C$_6$H$_3$}Co(CO)$_2$ (1e). In a glovebox, 1,3-$(Ph_2PO)_2C_6H_4$ (1.22 g, 2.55 mmol) dissolved in 20 mL of toluene was added dropwise to a Schlenk flask containing a solution of $Co_2(CO)_8$ (0.35 g, 1.02 mmol) in 15 mL of toluene. The flask was taken outside of the glovebox, connected to a Schlenk line, and heated with stirring at 110 °C for 24 h. The volatiles were removed under reduced pressure, and the red oily residue was washed first with pentane (20 mL, 10 mL × 2) and then with chilled (0 °C) methanol (1.5 mL × 3). The resulting solid was dried under vacuum to afford the product as a red powder (1.15 g, 95% yield). ^1H NMR (400 MHz, CD_2Cl_2, δ): 7.70−7.45 (m, Ar*H*, 20H), 6.89 (t, J_{H-H} = 7.8 Hz, Ar*H*, 1H), 6.64 (d, J_{H-H} = 7.8 Hz, Ar*H*, 2H). $^{13}C\{^1H\}$ NMR (101 MHz, C_6D_6, δ): 203.65 (t, J_{P-C} = 10.1 Hz, CO), 163.71 (t, J_{P-C} = 10.1 Hz, ArC), 138.81 (t, J_{P-C} = 25.3 Hz, ArC), 137.98 (t, J_{P-C} = 24.2 Hz, ArC), 131.08 (s, ArC), 131.00 (t, J_{P-C} = 7.1 Hz, ArC), 128.72 (t, J_{P-C} = 5.1 Hz, ArC), 126.4 (s, ArC), 106.33 (t, J_{P-C} = 8.1 Hz, ArC). $^{13}C\{^1H\}$ NMR (101 MHz, CD_2Cl_2, δ): 203.40 (m, CO), 163.09 (t, J_{P-C} = 9.9 Hz, ArC), 138.48 (t, J_{P-C} = 24.7 Hz, ArC), 137.52 (t, J_{P-C} = 24.4 Hz, ArC), 131.52 (s, ArC), 130.91 (t, J_{P-C} = 7.1 Hz, ArC), 128.91 (t, J_{P-C} = 5.3 Hz, ArC), 126.15 (s, ArC), 105.93 (t, J_{P-C} = 7.1 Hz, ArC). $^{31}P\{^1H\}$ NMR (162 MHz, C_6D_6, δ): 191.41 (s). $^{31}P\{^1H\}$ NMR (162 MHz, CD_2Cl_2, δ): 189.89 (s). Selected ATR-IR data (solid, cm^{-1}): 2001 (s, ν_{CO}), 1936 (s, ν_{CO}). Anal. Calcd for $C_{32}H_{23}O_4P_2Co$: C, 64.88; H, 3.91. Found: C, 65.13; H, 4.13.

Synthesis of {2,6-(^{t}Bu$_2$PO)$_2$C$_6$H$_3$}Co(CO) (2f). In a glovebox, a solution of 1,3-$(^tBu_2PO)_2C_6H_4$ (0.70 g, 1.76 mmol) in 20 mL of toluene was added dropwise to a Schlenk flask containing $Co_2(CO)_8$ (0.30 g, 0.88 mmol) predissolved in 15 mL of toluene. The flask was taken outside of the glovebox, connected to a Schlenk line, and heated with stirring at 110 °C for 36 h. After the mixture was cooled to room temperature, the volatiles were removed under vacuum. The resulting purple-red solid was treated with 40 mL of pentane and 60 mL of diethyl ether and then filtered through a pad of Celite. The filtrate was concentrated under vacuum to give a wine red solid, which was rinsed with chilled (−78 °C) methanol (6 mL × 2). The remaining solid was dried under vacuum to yield a red powder (0.50 g, 59% yield). The NMR and IR data matched with those reported in the literature.[16]

Synthesis of {2,6-(^{i}Pr$_2$PO)$_2$C$_6$H$_3$}Co(^{t}BuNC)(CO) (3a). Under an argon atmosphere, to a solution of $\{2,6\text{-}(^iPr_2PO)_2C_6H_3\}Co(CO)_2$ (100 mg, 0.22 mmol) in 15 mL of THF was added ^{t}BuNC (152 μL, 1.35 mmol). The resulting mixture was stirred at 50 °C for 24 h, at which point the mixture changed from yellow to orange. The volatiles were removed under reduced pressure, and the orange-yellow residue was washed with chilled (0 °C) methanol (0.5 mL × 3). The remaining solid was dried under vacuum to afford a yellow powder (40 mg), which was analyzed as a 4:1 mixture of **3a** and **4a**. A few single crystals of **3a** were obtained from a pentane solution of the mixture kept at −30 °C. ^1H NMR (400 MHz, C_6D_6, δ): 6.84−6.76 (m, Ar*H*, 3H), 2.46−2.36 (m, $CH(CH_3)_2$, 4H), 1.39−1.23 (m, $CH(CH_3)_2$, 24H), 0.88 (s, $C(CH_3)_3$, 9H). $^{13}C\{^1H\}$ NMR (101 MHz, C_6D_6, δ): 208.33 (m, CO), 165.81 (t, J_{P-C} = 9.1 Hz, ArC), 163.20 (m, CN^tBu), 140.71 (t, J_{P-C} = 23.7 Hz, ArC), 123.70 (s, ArC), 104.04 (t, J_{P-C} = 5.9 Hz, ArC), 55.33 (s, $C(CH_3)_3$), 32.90 (t, J_{P-C} = 11.6 Hz, $CH(CH_3)_2$), 32.51 (t, J_{P-C} = 10.6 Hz, $CH(CH_3)_2$), 30.25 (s, $C(CH_3)_3$), 17.82 (t, J_{P-C} = 2.5 Hz, $CH(CH_3)_2$), 17.59 (s, $CH(CH_3)_2$), 17.40 (s, $CH(CH_3)_2$), 17.32 (t, J_{P-C} = 2.5 Hz, $CH(CH_3)_2$). $^{31}P\{^1H\}$ NMR (162 MHz, C_6D_6, δ): 229.10 (s). Selected ATR-IR data (solid, cm^{-1}): 2092 (m), 2060 (m), 1899 (s, ν_{CO}).

Synthesis of {2,6-(^{i}Pr$_2$PO)$_2$C$_6$H$_3$}Co(^{t}BuNC)$_2$ (4a). Under an argon atmosphere, to a solution of $\{2,6\text{-}(^iPr_2PO)_2C_6H_3\}Co(CO)_2$ (0.50 g, 1.1 mmol) in 35 mL of THF was added ^{t}BuNC (0.75 mL, 6.6 mmol). The resulting mixture was stirred at 80 °C for 48 h, at which point the mixture changed from yellow to orange. The volatiles were removed under reduced pressure, and the orange-yellow residue was treated with 40 mL of pentane and filtered into another Schlenk flask via a cannula. The filtrate was concentrated under vacuum to give an orange solid, which was washed with chilled (0 °C) methanol (1.5 mL × 3). The remaining solid was dried under vacuum to afford the product as an orange fine powder (0.27 g, 43% yield). ^1H NMR (400 MHz, C_6D_6, δ): 6.82−6.76 (m, Ar*H*, 3H), 2.59−2.50 (m, $CH(CH_3)_2$, 4H), 1.47−1.42 (m, $CH(CH_3)_2$, 12H), 1.40−1.35 (m, $CH(CH_3)_2$, 12H), 1.00 (s, $C(CH_3)_3$, 18H). $^{13}C\{^1H\}$ NMR (101 MHz, C_6D_6, δ): 172.69 (m, CN^tBu), 165.55 (t, J_{P-C} = 11.1 Hz, ArC), 143.09 (t, J_{P-C} = 25.3 Hz, ArC), 122.34 (s, ArC), 103.51 (t, J_{P-C} = 6.1 Hz, ArC), 54.82 (s, $C(CH_3)_3$), 33.11 (t, J_{P-C} = 9.1 Hz, $CH(CH_3)_2$), 30.79 (s, $C(CH_3)_3$), 18.20 (t, J_{P-C} = 3.1 Hz, $CH(CH_3)_2$), 18.17 (s, $CH(CH_3)_2$). $^{31}P\{^1H\}$ NMR (162 MHz, C_6D_6, δ): 225.93 (s). Selected ATR-IR data (solid, cm^{-1}): 2077 (m), 2043 (m), 1912 (m, br). Anal. Calcd for $C_{28}H_{49}N_2O_2P_2Co$: C, 59.36; H, 8.72; N, 4.94. Found: C, 58.80; H, 8.81; N, 4.82.

General Procedure for the Catalytic Hydrosilylation of Aldehydes. To a 50 mL Schlenk flask were added **1b** (10 mg, 0.020 mmol), an aldehyde (2.0 mmol), $(EtO)_3SiH$ (406 μL, 2.2 mmol), and 2 mL of THF. The resulting mixture was exposed to a Schlenk line filled with argon and stirred at 50 °C for 12 h. The reaction mixture was then quenched with a 10% aqueous solution of NaOH (∼5 mL) and stirred vigorously at 50 °C for 24 h. The organic product was extracted with Et_2O (20 mL × 3) or CH_2Cl_2 (20 mL × 3, for products from 4-(dimethylamino)benzaldehyde and 2-naphthaldehyde), dried over anhydrous $MgSO_4$, and concentrated under vacuum. If needed, the alcohol product could be further purified by flash column chromatography (with 20% ethyl acetate in hexanes as eluent). The ^1H and $^{13}C\{^1H\}$ NMR spectra of the primary alcohol products are provided in the Supporting Information.

X-ray Structure Determinations. Single crystals of **1a**−**d**, **3a**, and **4a** were obtained from pentane solutions kept at −30 °C. Single crystals of **1e** were obtained from a THF solution kept at −30 °C. Crystal data collection and refinement parameters are provided in the Supporting Information. Intensity data for **1a**,**e** were collected at 150 K on a Bruker PHOTON100 CMOS detector at Beamline 11.3.1 at the Advanced Light Source (Lawrence Berkeley National Laboratory) using synchrotron radiation tuned to λ = 0.7749 Å. Intensity data for **1b**,**d** were collected at 150 K on a Bruker APEX-II CCD

DOI: 10.1021/acs.organomet.8b00273
Organometallics XXXX, XXX, XXX−XXX

diffractometer using graphite-monochromated Mo Kα radiation (λ = 0.71073 Å). Intensity data for **1c**, **3a**, and **4a** were collected at 150 K on a Bruker D8 Venture Mo-IμS Photon-II diffractometer (λ = 0.71073 Å). The data frames were processed using the program SAINT. The data were corrected for decay, Lorentz, and polarization effects as well as absorption and beam corrections on the basis of the multiscan technique. The structures were solved by a combination of direct methods in SHELXTL and the difference Fourier technique and refined by full matrix least squares on F^2. Non-hydrogen atoms were refined with anisotropic displacement parameters. H atoms were calculated and treated with a riding model. No solvent of crystallization is present in the lattice for any of the structures. Two independent molecules of **1b** were found in the unit cell. In **1c**, one isopropyl group is disordered and was refined with a two-component disorder model. The crystal structures for **1a**−**e**, **3a**, and **4a** have been deposited at the Cambridge Crystallographic Data Centre (CCDC) and allocated the deposition numbers CCDC 1839889 − 1839895.

■ ASSOCIATED CONTENT

Supporting Information

The Supporting Information is available free of charge on the ACS Publications website at DOI: 10.1021/acs.organomet.8b00273.

NMR and IR spectra of the cobalt complexes, NMR spectra of alcohols isolated from the catalytic reactions, and X-ray crystallographic information for **1a**−**e**, **3a**, and **4a** (PDF)

Optimized Cartesian coordinates for compounds **1a**−**e**, **3a**, and **4a** (MOL)

Accession Codes

CCDC 1839889−1839895 contain the supplementary crystallographic data for this paper. These data can be obtained free of charge via www.ccdc.cam.ac.uk/data_request/cif, or by emailing data_request@ccdc.cam.ac.uk, or by contacting The Cambridge Crystallographic Data Centre, 12 Union Road, Cambridge CB2 1EZ, UK; fax: +44 1223 336033.

■ AUTHOR INFORMATION

Corresponding Author

*E-mail for H.G.: hairong.guan@uc.edu.

ORCID

Hairong Guan: 0000-0002-4858-3159

Notes

The authors declare no competing financial interest.

■ ACKNOWLEDGMENTS

We thank the National Science Foundation (CHE-1464734) for support of this research. Crystallographic data were collected on a Bruker APEX-II CCD diffractometer (funded by NSF-MRI grant CHE-0215950), on a Bruker D8 Venture diffractometer (funded by NSF-MRI grant CHE-1625737), or through the SCrALS (Service Crystallography at Advanced Light Source) Program at Beamline 11.3.1 at the Advanced Light Source (ALS), Lawrence Berkeley National Laboratory (supported by the U.S. Department of Energy, Office of Basic Energy Sciences, under contract No. DE-AC02-05CH11231).

■ REFERENCES

(1) (a) Morales-Morales, D. *Mini-Rev. Org. Chem.* **2008**, *5*, 141−152. (b) Zargarian, D.; Castonguay, A.; Spasyuk, D. M. *Top. Organomet. Chem.* **2013**, *40*, 131−174. (c) Adhikary, A.; Guan, H. *ACS Catal.* **2015**, *5*, 6858−6873. (d) Murugesan, S.; Kirchner, K. *Dalton Trans.* **2016**, *45*, 416−439.

(2) (a) Choi, J.; MacArthur, A. H. R.; Brookhart, M.; Goldman, A. S. *Chem. Rev.* **2011**, *111*, 1761−1779. (b) Haibach, M. C.; Kundu, S.; Brookhart, M.; Goldman, A. S. *Acc. Chem. Res.* **2012**, *45*, 947−958. (c) Kumar, A.; Bhatti, T. M.; Goldman, A. S. *Chem. Rev.* **2017**, *117*, 12357−12384.

(3) (a) Szabó, K. J. *Synlett* **2006**, *2006*, 811−824. (b) Selander, N.; Szabó, K. J. *Chem. Rev.* **2011**, *111*, 2048−2076.

(4) Timpa, S. D.; Pell, C. J.; Ozerov, O. V. *J. Am. Chem. Soc.* **2014**, *136*, 14772−14779.

(5) Chakraborty, S.; Bhattacharya, P.; Dai, H.; Guan, H. *Acc. Chem. Res.* **2015**, *48*, 1995−2003.

(6) (a) Chakraborty, S.; Zhang, J.; Krause, J. A.; Guan, H. *J. Am. Chem. Soc.* **2010**, *132*, 8872−8873. (b) Chakraborty, S.; Patel, Y. J.; Krause, J. A.; Guan, H. *Polyhedron* **2012**, *32*, 30−34. (c) Chakraborty, S.; Zhang, J.; Patel, Y. J.; Krause, J. A.; Guan, H. *Inorg. Chem.* **2013**, *52*, 37−47.

(7) Chakraborty, S.; Patel, Y. J.; Krause, J. A.; Guan, H. *Angew. Chem., Int. Ed.* **2013**, *52*, 7523−7526.

(8) Bhattacharya, P.; Krause, J. A.; Guan, H. *J. Am. Chem. Soc.* **2014**, *136*, 11153−11161.

(9) (a) Göttker-Schnetmann, I.; White, P.; Brookhart, M. *J. Am. Chem. Soc.* **2004**, *126*, 1804−1811. (b) Morales-Morales, D.; Redón, R.; Yung, C.; Jensen, C. M. *Inorg. Chim. Acta* **2004**, *357*, 2953−2956. (c) Arunachalampillai, A.; Olsson, D.; Wendt, O. F. *Dalton Trans.* **2009**, 8626−8630. (d) Jonasson, K. J.; Ahlsten, N.; Wendt, O. F. *Inorg. Chim. Acta* **2011**, *379*, 76−80. (e) Brück, A.; Gallego, D.; Wang, W.; Irran, E.; Driess, M.; Hartwig, J. F. *Angew. Chem., Int. Ed.* **2012**, *51*, 11478−11482. (f) Lao, D. B.; Owens, A. C. E.; Heinekey, D. M.; Goldberg, K. I. *ACS Catal.* **2013**, *3*, 2391−2396. (g) Goldberg, J. M.; Wong, G. W.; Brastow, K. E.; Kaminsky, W.; Goldberg, K. I.; Heinekey, D. M. *Organometallics* **2015**, *34*, 753−762. (h) Mucha, N. T.; Waterman, R. *Organometallics* **2015**, *34*, 3865−3872. (i) Press, L. P.; Kosanovich, A. J.; McCulloch, B. J.; Ozerov, O. V. *J. Am. Chem. Soc.* **2016**, *138*, 9487−9497. (j) Polukeev, A. V.; Wendt, O. F. *Organometallics* **2017**, *36*, 639−649.

(10) (a) Salem, H.; Shimon, L. J. W.; Leitus, G.; Weiner, L.; Milstein, D. *Organometallics* **2008**, *27*, 2293−2299. (b) Polezhaev, A. V.; Kuklin, S. A.; Ivanov, D. M.; Petrovskii, P. V.; Dolgushin, F. M.; Ezernitskaya, M. G.; Koridze, A. A. *Russ. Chem. Bull.* **2009**, *58*, 1847−1854. (c) Timpa, S. D.; Fafard, C. M.; Herbert, D. E.; Ozerov, O. V. *Dalton Trans.* **2011**, *40*, 5426−5429. (d) Pell, C. J.; Ozerov, O. V. *ACS Catal.* **2014**, *4*, 3470−3480.

(11) (a) Wang, Z.; Sugiarti, S.; Morales, C. M.; Jensen, C. M.; Morales-Morales, D. *Inorg. Chim. Acta* **2006**, *359*, 1923−1928. (b) Takaya, H.; Iwaya, T.; Ogata, K.; Isozaki, K.; Yokoi, T.; Yoshida, R.; Yasuda, N.; Seike, H.; Takenaka, T.; Nakamura, M. *Synlett* **2013**, *24*, 1910−1914. (c) Anderson, B. G.; Spencer, J. L. *Chem. - Eur. J.* **2014**, *20*, 6421−6432. (d) Solano-Prado, M. A.; Estudiante-Negrete, F.; Morales-Morales, D. *Polyhedron* **2010**, *29*, 592−600. (e) Espinosa-Jalapa, N. Á.; Hernández-Ortega, S.; Le Goff, X.-F.; Morales-Morales, D.; Djukic, J.-P.; Le Lagadec, R. *Organometallics* **2013**, *32*, 2661−2673. (f) Joksch, M.; Haak, J.; Spannenberg, A.; Beweries, T. *Eur. J. Inorg. Chem.* **2017**, *2017*, 3815−3822. (g) Joksch, M.; Agarwala, H.; Haak, J.; Spannenberg, A.; Beweries, T. *Polyhedron* **2018**, *143*, 118−125.

(12) (a) Morales-Morales, D.; Grause, C.; Kasaoka, K.; Redón, R.; Cramer, R. E.; Jensen, C. M. *Inorg. Chim. Acta* **2000**, *300*−*302*, 958−963. (b) Wallner, O. A.; Szabó, K. J. *Org. Lett.* **2004**, *6*, 1829−1831. (c) Gong, J.-F.; Zhang, Y.-H.; Song, M.-P.; Xu, C. *Organometallics* **2007**, *26*, 6487−6492. (d) Polukeev, A. V.; Kuklin, S. A.; Petrovskii, P. V.; Peregudova, S. M.; Smol'yakov, A. F.; Dolgushin, F. M.; Koridze, A. A. *Dalton Trans.* **2011**, *40*, 7201−7209. (e) Adhikary, A.; Schwartz, J. R.; Meadows, L. M.; Krause, J. A.; Guan, H. *Inorg. Chem. Front.* **2014**, *1*, 71−82. (f) Lee, G. M.; Korobkov, I.; Baker, R. T. *J. Organomet. Chem.* **2017**, *847*, 270−277.

(13) (a) Gómez-Benítez, V.; Baldovino-Pantaleón, O.; Herrera-Álvarez, C.; Toscano, R. A.; Morales-Morales, D. *Tetrahedron Lett.* **2006**, *47*, 5059−5062. (b) Pandarus, V.; Zargarian, D. *Chem. Commun.* **2007**, 978−980. (c) Pandarus, V.; Zargarian, D. *Organo-*

DOI: 10.1021/acs.organomet.8b00273
Organometallics XXXX, XXX, XXX−XXX

metallics **2007**, *26*, 4321−4334. (d) Chakraborty, S.; Krause, J. A.; Guan, H. *Organometallics* **2009**, *28*, 582−586. (e) Castonguay, A.; Spasyuk, D. M.; Madern, N.; Beauchamp, A. L.; Zargarian, D. *Organometallics* **2009**, *28*, 2134−2141. (f) Salah, A. B.; Zargarian, D. *Dalton Trans.* **2011**, *40*, 8977−8985. (g) Chen, T.; Yang, L.; Li, L.; Huang, K.-W. *Tetrahedron* **2012**, *68*, 6152−6157. (h) Vabre, B.; Lambert, M. L.; Petit, A.; Ess, D. H.; Zargarian, D. *Organometallics* **2012**, *31*, 6041−6053. (i) Vabre, B.; Spasyuk, D. M.; Zargarian, D. *Organometallics* **2012**, *31*, 8561−8570. (j) Estudiante-Negrete, F.; Hernández-Ortega, S.; Morales-Morales, D. *Inorg. Chim. Acta* **2012**, *387*, 58−63. (k) Jonasson, K. J.; Wendt, O. F. *Chem. - Eur. J.* **2014**, *20*, 11894−11902. (l) Lapointe, S.; Vabre, B.; Zargarian, D. *Organometallics* **2015**, *34*, 3520−3531. (m) Adhikary, A.; Krause, J. A.; Guan, H. *Organometallics* **2015**, *34*, 3603−3610. (n) García-Eleno, M. A.; Padilla-Mata, E.; Estudiante-Negrete, F.; Pichal-Cerda, F.; Hernández-Ortega, S.; Toscano, R. A.; Morales-Morales, D. *New J. Chem.* **2015**, *39*, 3361−3365. (o) Salah, A.; Corpet, M.; Khan, N. u.-H.; Zargarian, D.; Spasyuk, D. M. *New J. Chem.* **2015**, *39*, 6649−6658. (p) Li, H.; Meng, W.; Adhikary, A.; Li, S.; Ma, N.; Zhao, Q.; Yang, Q.; Eberhardt, N. A.; Leahy, K. M.; Krause, J. A.; Zhang, J.; Chen, X.; Guan, H. *J. Organomet. Chem.* **2016**, *804*, 132−141.

(14) Hebden, T. J.; St. John, A. J.; Gusev, D. G.; Kaminsky, W.; Goldberg, K. I.; Heinekey, D. M. *Angew. Chem., Int. Ed.* **2011**, *50*, 1873−1876.

(15) A closely related cobalt pincer complex $\{2,6\text{-}(^{t}Bu_2PNH)_2C_6H_3\}$CoCl was obtained in 32% yield from cyclometalation of 1,3-$(^{t}Bu_2PNH)_2C_6H_4$ with $CoCl_2$. For details, see: Murugesan, S.; Stöger, B.; Weil, M.; Veiros, L. F.; Kirchner, K. *Organometallics* **2015**, *34*, 1364−1372.

(16) Guard, L. M.; Hebden, T. J.; Linn, D. E., Jr.; Heinekey, D. M. *Organometallics* **2017**, *36*, 3104−3109.

(17) van der Zeijden, A. A. H.; van Koten, G. *Inorg. Chem.* **1986**, *25*, 4723−4725.

(18) Kent, M. A.; Woodall, C. H.; Haddow, M. F.; McMullin, C. L.; Pringle, P. G.; Wass, D. F. *Organometallics* **2014**, *33*, 5686−5692.

(19) Lithiation was performed directly to 1,3-$(^{i}Pr_2PNMe)_2C_6H_4$ without introducing a halide to the pincer ligand. For details, see: Murugesan, S.; Stöger, B.; Carvalho, M. D.; Ferreira, L. P.; Pittenauer, E.; Allmaier, G.; Veiros, L. F.; Kirchner, K. *Organometallics* **2014**, *33*, 6132−6140.

(20) Zhang, J.; Medley, C. M.; Krause, J. A.; Guan, H. *Organometallics* **2010**, *29*, 6393−6401.

(21) (a) Xu, G.; Sun, H.; Li, X. *Organometallics* **2009**, *28*, 6090−6095. (b) Huang, S.; Zhao, H.; Li, X.; Wang, L.; Sun, H. *RSC Adv.* **2015**, *5*, 15660−15667.

(22) Though not a POCOP pincer complex, $(^{Ph}P^{N}C^{N}P)Co(PMe_3)_2$ ($^{Ph}P^{N}C^{N}P$ = bis(1-diphenylphosphino-1*H*-pyrrol-2-yl)methyl) was also prepared from C−H bond activation of the ligand with $MeCo(PMe_3)_4$. For details, see: (a) Zhu, G.; Li, X.; Xu, G.; Wang, L.; Sun, H. *Dalton Trans.* **2014**, *43*, 8595−8598. (b) Zhu, G.; Wang, L.; Sun, H.; Li, X. *RSC Adv.* **2015**, *5*, 19402−19408.

(23) Lian, Z.; Xu, G.; Li, X. *Acta Crystallogr., Sect. E: Struct. Rep. Online* **2010**, *66*, m636.

(24) Roddick, D. M. *Top. Organomet. Chem.* **2013**, *40*, 49−88.

(25) Murahashi, S. *J. Am. Chem. Soc.* **1955**, *77*, 6403−6404.

(26) Murahashi, S.; Horiie, S. *J. Am. Chem. Soc.* **1956**, *78*, 4816−4817.

(27) Hosokawa, S.; Ito, J.; Nishiyama, H. *Organometallics* **2013**, *32*, 3980−3985.

(28) $Co_2(CO)_8$ purchased from Sigma-Aldrich is moistened with a variable amount of hexane (1−10%) as a stabilizer. Our product yields are likely underestimated because the amount of hexane was not considered in our calculations.

(29) Sternberg, H. W.; Wender, I.; Orchin, M. *Anal. Chem.* **1952**, *24*, 174−176.

(30) Addison, A. W.; Rao, T. N.; Reedijk, J.; van Rijn, J.; Verschoor, G. C. *J. Chem. Soc., Dalton Trans.* **1984**, 1349−1356.

(31) (a) Bhattacharya, P.; Krause, J. A.; Guan, H. *Organometallics* **2011**, *30*, 4720−4729. (b) Bhattacharya, P.; Krause, J. A.; Guan, H. *Organometallics* **2014**, *33*, 6113−6121.

(32) Wang, W.; Gu, P.; Wang, Y.; Wei, H. *Organometallics* **2014**, *33*, 847−857.

(33) For representative reviews on catalytic hydrosilylation of carbonyl functionalities, see: (a) Díez-González, S.; Nolan, S. P. *Acc. Chem. Res.* **2008**, *41*, 349−358. (b) Zhang, M.; Zhang, A. *Appl. Organomet. Chem.* **2010**, *24*, 751−757. (c) Junge, K.; Schröder, K.; Beller, M. *Chem. Commun.* **2011**, *47*, 4849−4859. (d) Le Bailly, B. A. F.; Thomas, S. P. *RSC Adv.* **2011**, *1*, 1435−1445. (e) Trovitch, R. J. *Synlett* **2014**, *25*, 1638−1642. (f) Trovitch, R. J. *Acc. Chem. Res.* **2017**, *50*, 2842−2852.

(34) (a) Brunner, H.; Amberger, K. *J. Organomet. Chem.* **1991**, *417*, C63−C65. (b) Inagaki, T.; Phong, L. T.; Furuta, A.; Ito, J.; Nishiyama, H. *Chem. - Eur. J.* **2010**, *16*, 3090−3096. (c) Yu, F.; Zhang, X.-C.; Wu, F.-F.; Zhou, J.-N.; Fang, W.; Wu, J.; Chan, A. S. C. *Org. Biomol. Chem.* **2011**, *9*, 5652−5654. (d) Sauer, D. C.; Wadepohl, H.; Gade, L. H. *Inorg. Chem.* **2012**, *51*, 12948−12958. (e) Niu, Q.; Sun, H.; Li, X.; Klein, H.-F.; Flörke, U. *Organometallics* **2013**, *32*, 5235−5238. (f) Scheuermann, M. L.; Semproni, S. P.; Pappas, I.; Chirik, P. J. *Inorg. Chem.* **2014**, *53*, 9463−9465. (g) Zhou, H.; Sun, H.; Zhang, S.; Li, X. *Organometallics* **2015**, *34*, 1479−1486. (h) Nesbit, M. A.; Suess, D. L. M.; Peters, J. C. *Organometallics* **2015**, *34*, 4741−4752. (i) Smith, A. D.; Saini, A.; Singer, L. M.; Phadke, N.; Findlater, M. *Polyhedron* **2016**, *114*, 286−291.

(35) (a) Pearson, A. J.; Shively, R. J., Jr.; Dubbert, R. A. *Organometallics* **1992**, *11*, 4096−4104. (b) Casey, C. P.; Guan, H. *J. Am. Chem. Soc.* **2009**, *131*, 2499−2507. (c) Plank, T. N.; Drake, J. L.; Kim, D. K.; Funk, T. W. *Adv. Synth. Catal.* **2012**, *354*, 597−601.

(36) While C_6D_6 is a more affordable NMR solvent for mechanistic studies, THF was used for preparative-scale reactions due to its lower health score. A comparative study showed that the catalytic activity of **1b** in THF was similar to that in benzene. In contrast, MeCN, a solvent with lower safety and health scores, proved to be less effective for catalytic hydrosilylation of PhCHO (13% conversion over 12 h in the presence of 1 mol% of **1a**). For safety and health scores of different solvents, see: Prat, D.; Wells, A.; Hayler, J.; Sneddon, H.; McElroy, C. R.; Abou-Shehada, S.; Dunn, P. J. *Green Chem.* **2016**, *18*, 288−296.

(37) (a) Ingleson, M. J.; Pink, M.; Fan, H.; Caulton, K. G. *Inorg. Chem.* **2007**, *46*, 10321−10334. (b) Spentzos, A. Z.; Barnes, C. L.; Bernskoetter, W. H. *Inorg. Chem.* **2016**, *55*, 8225−8233. (c) Polezhaev, A. V.; Chen, C.-H.; Losovyj, Y.; Caulton, K. G. *Chem. - Eur. J.* **2017**, *23*, 8039−8050.

(38) Murugesan, S.; Stöger, B.; Pittenauer, E.; Allmaier, G.; Veiros, L. F.; Kirchner, K. *Angew. Chem., Int. Ed.* **2016**, *55*, 3045−3048.

(39) Mironov, M. A. General Aspects of Isocyanide Reactivity. In *Isocyanide Chemistry: Applications in Synthesis and Material Science*, 1st ed.; Nenajdenko, V. G., Ed.; Wiley-VCH: Weinheim, Germany, 2012; pp 35−73.

(40) (a) Widegren, J. A.; Finke, R. G. *J. Mol. Catal. A: Chem.* **2003**, *198*, 317−341. (b) Crabtree, R. H. *Chem. Rev.* **2012**, *112*, 1536−1554.

(41) Bedford, R. B.; Draper, S. M.; Scully, P. N.; Welch, S. L. *New J. Chem.* **2000**, *24*, 745−747.

DOI: 10.1021/acs.organomet.8b00273
Organometallics XXXX, XXX, XXX−XXX